Constraints imposed by the partial wave amplitudes on the decays of $J = 1, 2$ mesons

Vanamali Shastry[*] and Enrico Trotti[†]
Institute of Physics, Jan Kochanowski University, ul. Uniwersytecka 7, P-25-406 Kielce, Poland

Francesco Giacosa[‡]
Institute of Physics, Jan Kochanowski University, ul. Uniwersytecka 7, P-25-406 Kielce, Poland and Institute for Theoretical Physics, Johann Wolfgang Goethe–University, Max von Laue–Strasse 1 D-60438 Frankfurt, Germany

(Received 2 September 2021; accepted 14 February 2022; published 21 March 2022)

We study the two-body decays of mesons using the covariant helicity formalism. In particular, we show how the partial wave analysis of decays constrains the interacting terms entering the Lagrangian describing the decays of mesons with $J = 1$ and $J = 2$. We use available information on partial wave analysis to study specific mesonic decays and to make predictions for not yet measured quantities as well as to investigate the isoscalar mixing angle in the axial-vector, pseudovector and pseudotensor sectors. In particular, in the axial-vector sector our result agrees with the LHCb one, and in the pseudotensor sector we confirm a quite large (and negative) angle in the nonstrange-strange basis, which is compatible with a large contribute of the axial anomaly.

DOI: 10.1103/PhysRevD.105.054022

I. INTRODUCTION

The study of mesons and their decays can provide a wealth of information regarding the interactions between the various states as well as the internal dynamics of the states involved, and ultimately, the strong interactions.

On the experimental front, a lot of effort has been dedicated to the study of mesonic decays (e.g., Refs. [1–9]), as these decays are a way to generate and observe new states as well as portals to possible new physics. On the theoretical front too, a wealth of knowledge has been gained using various field theoretic models, quarks models, and effective field theories [10–14].

A vast majority of the phenomenological models formulated till date estimate the coupling constants by analyzing the mass of the mesons, their widths, and the branching fractions of their decays. One crucial set of data points available in the PDG, the ratio of the partial wave amplitudes (PWAs, see for instance Ref. [15]), is usually not taken into account. We demonstrate in the present work how this particular data can be used to build more robust field theoretic phenomenological models and to put a tighter constraint on their parameters.

In order to set the frame of our work, let us consider a decay of the type

$$A \to BC,$$

where A, B, C are certain mesonic fields with definite total spin J_A, J_B, and J_C. The corresponding interaction Lagrangian that describes this decay process should fulfill the basic constraint such as Lorentz as well as, for QCD processes, parity and charge-conjugation invariance. It can be expressed as

$$\mathcal{L}_{ABC} = \mathcal{L}^{\mathrm{c}}_{ABC} + \mathcal{L}^{\mathrm{d}}_{ABC} + \ldots \tag{1}$$

where $\mathcal{L}^{\mathrm{c}}_{ABC}$ contains the lowest possible number of derivatives, while $\mathcal{L}^{\mathrm{d}}_{ABC}$ is the next term with two additional derivatives, etc.

Various approaches, based on the realization of flavor symmetry or, more generally, on the linear realization of chiral symmetry consider the first term as dominant, e.g., Refs. [16–21], while approaches based on the nonlinear realization of chiral symmetry typically contain terms with higher derivatives (see for instance, Refs. [22–28]).

An important aspect of the decays $A \to B + C$ is that different waves for the final product are possible. Denoting with ℓ the relative orbital angular momentum between

[*]vanamalishastry@gmail.com
[†]trottienrico@gmail.com
[‡]fgiacosa@ujk.edu.pl

B and C, the possible values of ℓ range between $|J_A - (J_B + J_C)|$ up to $J_A + (J_B + J_C)$. For instance, in the decay $a_1(1260) \to \rho\pi$ the waves $\ell = 0$ and $\ell = 2$ are allowed, while in the $\pi_2(1670) \to f_2(1270)\pi$ decay one may have $\ell = 0, 2, 4$. The ratio between two allowed ℓ-values can be determined by an appropriate PWA analysis [1].

A natural question regards the connection of the interaction terms in Eq. (1) to the ratio of partial waves. In general, each interaction Lagrangian gives a nonzero contribution to each partial wave. For instance, one may ask for a certain decay if the term with the lowest number of derivatives is sufficient do describe data or not. Conversely, the possibility that the derivative interaction term dominates can be also addressed.

In this work, we study, in a systematic framework, the PWA of the decays of the axial-vector, pseudovector, and pseudotensor mesons by using model Lagrangian(s) of the type of Eq. (1). Our aim is to understand the role played by the various interactions in the decays of these mesons. Within this respect, the information gained by PWA turns out to be very useful. We thus can—on the one hand—reproduce previous results on the subject (in particular Ref. [29], in which also a model Lagrangian was used), and on the other hand, extend the procedure to the whole class of unstable high-spin mesons mentioned above. Moreover, we shall analyze (to our knowledge for the first time using PWA) the mixing in the isoscalar sector of the investigated mesonic nonets. Namely, the question about the role of the anomaly, besides the well-known case of the pseudoscalar sector, is on its own an interesting aspect of nonperturbative QCD [30–32].

Our results about the PWA shall be compared to those of other approaches, such as the PWA analysis of the $^3P_0$ model and the lattice calculations. We find that our results agree with those of the $^3P_0$ model in the $J = 1$ sector [33]. On the lattice front, the $b_1(1235) \to \omega\pi$ decay was studied by the Hadron Spectrum collaboration recently [34]. Their inference that the $b_1(1235)$ couples strongly to the S–wave $\omega\pi$ compared to the D–wave is in line with experimental results [1].

This paper is organized into four sections. In Sec. II, we discuss the formalism used in deriving the PWAs and the construction of the polarization tensors. In Sec. III we derive the partial wave amplitudes for the different decays discussed in the paper, and analyze their behavior. In Sec. IV, we discuss the results of the work and their consequences. Finally, we summarize the entire work in Sec. V.

II. PARTIAL WAVE AMPLITUDES

Much research has been conducted on the partial wave decomposition of the decay processes. One of the earliest works in this direction was the tensor formalism by Zemach [35,36]. In this formalism, the decay amplitude is written in terms of the noncovariant 3-dimensional spin tensors defined in the rest frame of each decaying particle. This results in a *frame dependent* decay width which leads to hurdles in interpreting the square of the amplitude as the decay probability.

An alternative approach to analyzing the partial waves is the helicity formalism. Initiated by Jacob and Wick [37], the helicity formalism has been used extensively to study the decay processes. In this formalism, the angular dependence of the decay process is captured in the Wigner D-matrices $D^J_{mm'}$. The remaining part of the decay amplitude forms the helicity coupling amplitude. In a typical scenario, where experimental data has to be analyzed, the helicity amplitudes are constructed empirically using the Breit-Wigner functions and the centrifugal functions—which are nothing but the moduli of the Zemach tensors. This approach makes the formalism noncovariant, making it unsuitable for practical applications as the decay amplitude must be a Lorentz invariant.

Chung proposed a covariant form of the helicity formalism in which the helicity coupling amplitude is constructed from the polarization tensors and hence is a function of the ratio E/m (E and m are the energy and mass of the particles involved in the decay process, as measured in the rest frame of the parent) making it a Lorentz scalar [38,39]. In the present work, we make use of model Lagrangians to write down the amplitude of the decays. We then derive the helicity coupling amplitudes from the decay amplitudes which we find to be functions of the energy (or 3–momentum) of the daughter mesons and rest masses of the mesons involved, as measured in the rest frame of the parent.

In the following subsection, we discuss briefly the covariant helicity formalism.

A. The covariant helicity formalism

Consider the two-body decay process, $A \to BC$. Let the total angular momentum states of the particles A, B, and C be $|J, M_J\rangle$, $|s, \lambda\rangle$, and $|\sigma, \nu\rangle$ respectively. Also, let the sum of the total spin quantum numbers of the daughter states be given by S, i.e.,

$$|S, m_s\rangle = |s, \lambda\rangle \oplus |\sigma, \nu\rangle, \tag{2}$$

where $\oplus$ implies that the $|S, m_s\rangle$ state is constructed from $|s, \lambda\rangle$ and $|\sigma, \nu\rangle$ by following the rules of addition of the angular momenta. The spin of the parent can then be constructed by adding the total spin of the daughters with the relative orbital angular momentum (ℓ) carried by them, i.e.,

$$|J, M_J\rangle = |\ell, m_\ell\rangle \oplus |S, m_s\rangle. \tag{3}$$

Thus, unlike a two-body scattering process where an infinity of angular momentum channels are available, the number of angular momentum channels available for

a two-body decay is limited by the spins of the parent and daughter states. The value of ℓ must satisfy the condition that $J \in [|\ell - S|, \ell + S]$. Also, since we are interested only in the strong decays, an additional constraint of parity conservation has to be imposed. This determines if ℓ has to be even or odd (for a given value of S), further reducing the available number of angular momentum channels.

The amplitude for a two-body decay can be written as

$$\mathcal{M}^J(\theta, \phi; M_J) \propto D^{J*}_{M\delta}(\phi, \theta, 0) F^J_{\lambda\nu}, \tag{4}$$

where $D^{J*}_{M\delta}(\phi, \theta, 0)$ is the complex conjugate of the Wigner D–matrix, $F^J_{\lambda\nu}$ is the helicity amplitude, and $\delta = \lambda - \nu$. Equation (4) is a general result, and any model dependence will appear in the exact form of the helicity amplitudes. As a special case, if the frame of reference is such that the decay products are aligned along the $\pm z$–axis, the decay amplitude becomes proportional to only the helicity amplitude:

$$\mathcal{M}^J_{\lambda\delta}(0, 0; M_J) \propto F^J_{\lambda\nu}. \tag{5}$$

When the decay products are massive, the helicity amplitudes can be expanded in terms of the ℓS coupling amplitudes ($G^J_{\ell S}$) through the relation

$$F^J_{\lambda\nu} = \sum_{\ell S} \sqrt{\frac{2\ell + 1}{2J + 1}} \langle \ell 0 S\delta | J\delta \rangle \langle s\lambda\sigma - \nu | S\delta \rangle G^J_{\ell S}, \tag{6}$$

where $\langle \cdots | \cdots \rangle$ represent the Clebsch-Gordan coefficients. As explained above, the allowed values of ℓ are determined by the spin and parity of the parent and the decay products.

Some comments regarding the validity of the above relation are in order. First, the ℓS coupling amplitudes can be chosen in two ways: (i) empirically, by using the rule $G^J_{\ell S} \propto |\vec{k}|^\ell$, where $|\vec{k}|$ is the magnitude of the break-up momentum; (ii) from the polarization vectors. In the former case, the helicity amplitudes become noncovariant due to the frame dependence introduced by the choice of $G^J_{\ell S}$. The helicity amplitudes can be made Lorentz scalar using the latter method, if the polarization vectors are boosted to the appropriate frame [39,40]. The ratio of $G^J_{\ell S}$ gives us the ratio of the partial wave amplitudes.

Alternatively, one can expand the decay amplitude in terms of the spherical harmonics as

$$i\mathcal{M}(\theta, \phi; M_J) = i \sum_{\ell} \sum_{m_\ell = -\ell}^{\ell} G_\ell \langle \ell m_\ell S m_s | J M_J \rangle Y_{\ell m_\ell}(\theta, \phi). \tag{7}$$

The PWAs so derived will be proportional to the PWAs derived using the covariant helicity formalism, i.e.,

$$G_\ell = \sqrt{\frac{\alpha}{(2J + 1)}} G^J_{\ell S}, \tag{8}$$

where α is a numerical factor dependent on the normalization of the spherical harmonics. For the normalization $\int d\Omega |Y_{\ell m_\ell}|^2 = 1$, $\alpha = 4\pi$. The advantage of using the covariant helicity formalism is that, by choosing the helicity amplitudes suitably, we obtain

$$\sum_{\ell S} |G^J_{\ell S}|^2 = \sum_{\text{spins}} |\mathcal{M}|^2. \tag{9}$$

B. Polarization states

The present study is concerned with the decay of mesons with $J \geq 1$ in to states with one of them having $J \geq 1$. We detail the construction of the polarization vectors (PV) and polarization tensors (PT) in this subsection.

The PVs of a spin–1 state in its rest frame are given by

$$\begin{aligned} \epsilon^\mu(\vec{0}, +1) &= -\frac{1}{\sqrt{2}} \Big(0, 1, i, 0 \Big), \\ \epsilon^\mu(\vec{0}, -1) &= \frac{1}{\sqrt{2}} \Big(0, 1, -i, 0 \Big), \\ \epsilon^\mu(\vec{0}, 0) &= \Big(0, 0, 0, 1 \Big). \end{aligned} \tag{10}$$

These PVs satisfy the following orthonormality conditions:

$$k_\mu \epsilon^\mu(\vec{k}, m) = 0 \tag{11}$$

$$\epsilon^*_\mu(\vec{k}, m) \epsilon^\mu(\vec{k}, m') = -\delta_{mm'}. \tag{12}$$

Further, the projection operator is given by the identity

$$\tilde{g}_{\mu\nu} = \sum_m \epsilon_\mu(\vec{k}, m) \epsilon^*_\nu(\vec{k}, m) = -g_{\mu\nu} + \frac{k_\mu k_\nu}{M_0^2}, \tag{13}$$

where k_μ and M_0 are the 4-momentum and mass of the corresponding state respectively. The PTs for higher spin states can be constructed from the PVs using a standard algorithm. The PTs for a spin-J state can be constructed using the master formula

$$\begin{aligned} \epsilon^{\mu_1 \mu_2 \ldots \mu_J}(\vec{0}, m) = \sum_{m_1 m_2 \ldots} & \langle 1 m_1 1 m_2 | 2 n_1 \rangle \langle 2 n_1 1 m_3 | 3 n_2 \rangle \ldots \\ & \times \langle J - 1 n_{J-2} 1 m_J | J m \rangle \\ & \otimes \epsilon^{\mu_1}(\vec{0}, m_1) \epsilon^{\mu_2}(\vec{0}, m_2) \ldots \epsilon^{\mu_J}(\vec{0}, m_J). \end{aligned} \tag{14}$$

The states constructed using this algorithm satisfy the following orthonormality relations:

$$k_{\mu_i}\epsilon^{\mu_1\mu_2\cdots\mu_J}(m) = 0 \tag{15}$$

$$\epsilon^*_{\mu_1\mu_2\ldots\mu_J}(m)\epsilon^{\mu_1\mu_2\cdots\mu_J}(m') = (-1)^J\delta_{mm'} \tag{16}$$

and transform under rotations as

$$\epsilon^{\mu_1\mu_2\cdots\mu_J}(m) \to \sum_m{}'\epsilon^{\mu_1\mu_2\cdots\mu_J}(m')D^J_{m'm}(\phi,\theta,\psi). \tag{17}$$

We list below the explicit expressions for spin–2 states:

$$\epsilon^{\mu\nu}(\vec{k},+2) = \epsilon^{\mu}(\vec{k},+1)\epsilon^{\nu}(\vec{k},+1) \tag{18}$$

$$\epsilon^{\mu\nu}(\vec{k},+1) = \frac{1}{\sqrt{2}}[\epsilon^{\mu}(\vec{k},+1)\epsilon^{\nu}(\vec{k},0) + \epsilon^{\mu}(\vec{k},0)\epsilon^{\nu}(\vec{k},+1)] \tag{19}$$

$$\epsilon^{\mu\nu}(\vec{k},0) = \frac{1}{\sqrt{6}}[\epsilon^{\mu}(\vec{k},+1)\epsilon^{\nu}(\vec{k},-1) + \epsilon^{\mu}(\vec{k},-1)\epsilon^{\nu}(\vec{k},+1)] + \sqrt{\frac{2}{3}}\epsilon^{\mu}(\vec{k},0)\epsilon^{\nu}(\vec{k},0). \tag{20}$$

The PTs for states with $m = -1, -2$ can be obtained similarly by using the PVs with $m = -1$. The above definitions are valid for any particle moving with any 3-momentum $\vec{k}$ provided that the corresponding PVs are boosted appropriately before arriving at the PTs. Alternatively, one can construct the PTs using the PVs defined in the rest frame of the meson, and then boost the resultant PTs to the required frame.

III. DERIVING THE PWAs

In this section, we derive the PWAs for three decay processes *viz.,* $a_1(1260) \to \rho\pi$, $\pi_2(1670) \to f_2(1270)\pi$, and $\pi_2(1670) \to \rho\pi$. In principle, the following discussions can be extended to the decays of all the members of the corresponding nonets. The general results derived for the decay of the $a_1(1260)$ can also be extended to the decays of the $b_1(1235)$ meson.

A. The $a_1(1260) \to \rho\pi$ decay

The decay of the $a_1(1260)$ to $\rho\pi$ can be represented by the Lagrangian

$$\mathcal{L} = ig_c^A\langle a_{1,\mu}\rho^{\mu}\pi\rangle + ig_d^A\langle \mathfrak{a}_{1,\mu\nu}\rho^{\mu\nu}\pi\rangle, \tag{21}$$

where g_c^A and g_d^A are the coupling constants, and $\mathfrak{a}_{1,\mu\nu} = \partial_\mu a_{1,\nu} - \partial_\nu a_{1,\mu}$, $\rho^{\mu\nu} = \partial^\mu\rho^\nu - \partial^\nu\rho^\mu$ and $\langle\rangle$ represents trace over the isospin. The Lagrangian consists of two types of interactions[1]: local (contact) interactions and nonlocal (derivative) interactions. As we discuss in a while, the local interactions are sufficient to reproduce the D/S–ratio of the $a_1(1260) \to \rho\pi$ decay. We write down the full amplitude (including both interactions) as

$$\begin{aligned} i\mathcal{M} &= g_c^A\epsilon_\mu(0,M_J)\epsilon^{\mu*}(\vec{k},\lambda) + 2g_d^A[k_0\cdot k_1\epsilon^{\mu}(\vec{0},M_J)\epsilon^*_{\mu}(\vec{k_1},\lambda) \\ &\quad - k_0^\nu k_{1,\mu}\epsilon^{\mu}(\vec{0},M_J)\epsilon^*_{\nu}(\vec{k_1},\lambda)] \\ &= -\begin{cases} g_c^A + 2g_d^A M_{a_1}E_\rho & M_J = \lambda = \pm 1 \\ \gamma(g_c^A + 2g_d^A M_{a_1}E_\rho & \\ -2g_d^A M_{a_1}\beta k) & M_J = \lambda = 0 \end{cases}, \end{aligned} \tag{22}$$

where $k_0^\mu = (M_{a_1},\vec{0})$ is the 4-momentum of the decaying meson, $k_1^\mu = (E_\rho,0,0,k)$ is the 4-momentum of the vector decay product, M_{a_1} is the mass of the decaying meson, M_ρ and E_ρ are the mass and energy of the vector decay product respectively, and k is the magnitude of the 3-momentum carried by the vector decay product. Notice that the last term in the Eq. (22) contributes only when $M_J < |J|$. This statement is true for all the decays we have studied in this paper. The momentum dependence of the amplitude comes from the interaction terms as well as the polarization vectors. Thus, a simple Lagrangian with only contact interactions can also give rise to higher angular momentum partial waves in the amplitude, even though these higher partial waves will be suppressed. Conversely, derivative interaction may also lead to lowest-order partial wave contributions

We now proceed with the analysis of the $a_1(1260) \to \rho\pi$ decay. The permitted values for the angular momentum quantum number are $\ell = 0$ and 2. Hence, from Eq. (4),

$$F^1_{10} = \frac{1}{\sqrt{3}}G_0 + \frac{1}{\sqrt{6}}G_2 \tag{23}$$

$$F^1_{00} = \frac{1}{\sqrt{3}}G_0 - \sqrt{\frac{2}{3}}G_2, \tag{24}$$

where $G_0 = G^1_{01}$ and $G_2 = G^1_{21}$. We note that, if the helicity amplitudes $F^1_{10} = F^1_{00}$, then the decay is entirely due to the S–wave, and if $F^1_{00} = 2F^1_{10}$, the decay is entirely due to D–wave. From the amplitude [Eq. (22)], we see that

$$F^1_{10} = (g_c^A + 2g_d^A M_{a_1}E_\rho) \tag{25}$$

$$F^1_{00} = \gamma(g_c^A + 2g_d^A M_{a_1}E_\rho - 2g_d^A M_{a_1}\beta k) \tag{26}$$

(up to a common multiplier). Now, we can invert the above relations to get the PWAs as[2]

[1]Here, and in the following, we use the term "contact interactions" or "local interactions" to refer to operators without derivatives. Conversely, we call "derivative interactions" or "nonlocal interactions" for the other terms.

[2]Here, and everywhere else, the partial wave amplitudes are derived up to an overall phase since the ratios of the PWAs do not depend on them.

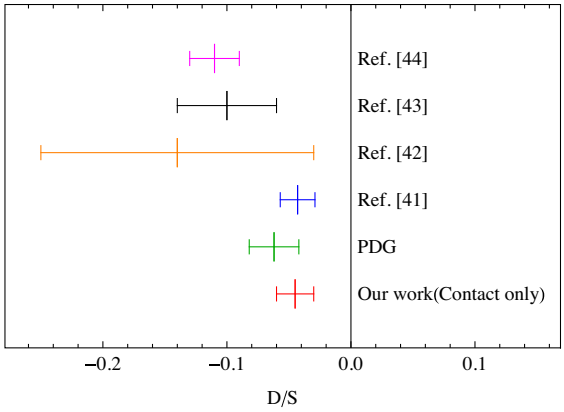

FIG. 1. D/S–ratio for the $a_1(1260) \to \rho\pi$ decay from various experiments and the uncertainties as listed in the PDG. For the sources of the values, see text.

$$G_2 = \sqrt{\frac{2}{3}}\left[g_c^A\left(\frac{M_\rho - E_\rho}{M_\rho}\right) + 2g_d^A M_{a_1}(E_\rho - M_\rho)\right] \quad (27)$$

$$G_0 = \frac{1}{\sqrt{3}}\left[g_c^A\left(\frac{2M_\rho + E_\rho}{M_\rho}\right) + 2g_d^A M_{a_1}(2E_\rho + M_\rho)\right]. \quad (28)$$

If we ignore the derivative interactions ($g_d^A = 0$), the ratio of the PWAs for the decay of $a_1(1260) \to \rho\pi$ is

$$\frac{G_2}{G_0} = \sqrt{2}\left(\frac{M_\rho - E_\rho}{2M_\rho + E_\rho}\right). \quad (29)$$

Since in any frame of reference other than the rest frame of the ρ–meson $E_\rho > M_\rho$, G_2 is negative, and hence $|G_2| < |G_0|$. Substituting the values of the masses of the mesons involved and the magnitude of the 3-momentum carried by the decay products, we get $G_2/G_0 = -0.045$, which is in good agreement with the value reported by the FOCUS collaboration [41] and within the error margin of the PDG value of -0.062 ± 0.02 [1]. In Fig. 1, we have shown the D/S–ratio for the $a_1(1260) \to \rho\pi$ decay obtained by various experiments along with the uncertainties compared to our work and the PDG average. Even when the derivative interactions are absent, our value is within the error estimate of the value obtained by the E852 collaboration ("Chung, 2002" [42]), and is in good agreement with that from the FOCUS experiment ("Link, 2007A" [41]). The values extracted by the OPAL collaboration ("Ackerstaff, 1997R" [43]) and the ARGUS ("Albrecht, 1993C" [44]) collaborations are significantly larger than our value. The experimental values and the corresponding uncertainties differ from each other significantly, as can be seen in Fig. 1. Hence, through out this study, we have used the PDG averages to estimate the parameters wherever needed.

The $a_1(1260)$ is a broad state with a width of 250–600 MeV [1]. Since it is close to the $\rho\pi$ threshold, the width of the unstable ρ–meson can significantly influence the width of the $a_1(1260) \to \rho\pi$ decay. This can be estimated by performing a spectral integration of the decay width. However, we find that the decay width does not change the qualitative picture (see the Appendix A for details).

Finally, the decay width is given by

$$\Gamma_{a_1\to\rho\pi} = f_{a_1\rho\pi}\frac{k}{24\pi M_{a_1}^2}\left[(g_c^A)^2\left(\frac{k^2}{M_\rho^2}+3\right) + 12 g_c^A g_d^A E_\rho M_{a_1} + 4(g_d^A)^2 M_{a_1}^2 M_\rho^2\left(\frac{2k^2}{M_\rho^2}+3\right)\right], \quad (30)$$

where $f_{a_1\rho\pi}$ is the isospin symmetry factor. The decay widths for the other members of the nonet can be obtained by using the corresponding values for the masses, energy, and isospin symmetry factor. The first term in the decay width arises purely from the contact interactions. The third term arises from the derivative interactions and adds to the contributions from the contact interactions. The second term is the interference between the contact and derivative interactions. The sign of g_d^A indicates that the contact and derivative interactions interfere destructively.

The ratios of the PWAs for the decays of the pseudovector mesons can be calculated via the expressions given in Eq. (27) and Eq. (28) by using the appropriate masses and energies. The $b_1(1235) \to \omega\pi$ decay is comparable to the $a_1(1260) \to \rho\pi$ decay, in that, the masses of the mesons involved and the 3-momenta carried by the decay products are nearly equal. Thus, one would expect the ratios of the PWAs to be nearly the same for both the decays. The Lagrangian with only contact interactions when extended to the $b_1(1235) \to \omega\pi$ decay, in fact, gives the value of the ratio as -0.043. However, the experimentally observed value is much different at 0.277 ± 0.027 [1].

This discrepancy can be addressed by including nonlocal interactions in the Lagrangian. The observed value of the magnitude of the D/S–ratio for the $b_1(1235) \to \omega\pi$ decay can be explained if the coupling constants have the ratio $g_d^B/g_c^B = -0.659\ \text{GeV}^{-2}$, as given the Table II (see also the discussions in Sec IV). We observe that this ratio is very close to $1/M_{b_1}^2$ in magnitude. Such a relation between the ratio of the coupling constants and the mass of the decaying state occurs in all the decays we have studied in this paper.

B. The $\pi_2(1670) \to f_2(1270)\pi$ decay

We introduce the following Lagrangian to describe the decay of the $\pi_2(1670)$ to $f_2(1270)\pi$

$$\mathcal{L} = \cos\beta_t(g_c^{PT}\langle\pi_{2,\mu\nu}f_2^{\mu\nu}\pi\rangle + g_d^{PT}\langle\pi_{2,\alpha\mu\nu}\mathfrak{f}_2^{\alpha\mu\nu}\pi\rangle), \quad (31)$$

where $\pi_{2,\alpha\mu\nu} = \partial_\alpha\pi_{2,\mu\nu} - \partial_\mu\pi_{2,\alpha\nu}$, $\mathfrak{f}_2^{\alpha\mu\nu} = \partial^\alpha f_2^{\mu\nu} - \partial^\mu f_2^{\alpha\nu}$, and $\beta_t(= 5.7°)$ is the angle of mixing between the 2^{++} iso-singlets [1] (already included for later convenience).

The experimental value of D/S–ratio for this decay is -0.18 ± 0.06 [1]. The amplitude for this decay is

$$\begin{aligned} i\mathcal{M} &= i\cos\beta_t [g_c^{PT}\epsilon_{\mu\nu}(\vec{0}, M_J)\epsilon^{\mu\nu *}(\vec{k}, \lambda) \\ &\quad + 2g_d^{PT}(k_0 \cdot k_1 \epsilon_{\mu\nu}(\vec{0}, M_J)\epsilon^{\mu\nu *}(\vec{k_1}, \lambda) \\ &\quad - k_{0,\alpha}k_1^{\nu}\epsilon_{\mu\nu}(\vec{0}, M_J)\epsilon^{\alpha\mu *}(\vec{k_1}, \lambda))] \end{aligned} \tag{32}$$

$$= i\cos\beta_t \begin{cases} g_c^{PT}\frac{(M_{f_2}^2+2E_{f_2}^2)}{3M_{f_2}^2} + 2g_d^{PT}\frac{M_{\pi_2}}{M_{f_2}^2}E_{f_2} & M_J = \lambda = 0 \\ g_c^{PT}\frac{E_{f_2}}{M_{f_2}} + g_d^{PT}\frac{M_{\pi_2}}{M_{f_2}}(k^2 + 2M_{f_2}^2) & M_J = \lambda = \pm 1 \\ g_c^{PT} + 2g_d^{PT}M_{\pi_2}E_{f_2} & M_J = \lambda = \pm 2 \end{cases}. \tag{33}$$

For the $\pi_2(1670) \to f_2(1270)\pi$ decay, the allowed values of the relative angular momentum are $\ell = 0, 2, 4$. Thus, from Eq. (4), we get

$$\begin{aligned} F_{20}^2 &= \frac{1}{\sqrt{5}}G_0 + \sqrt{\frac{2}{7}}G_2 + \frac{1}{\sqrt{70}}G_4 \\ F_{10}^2 &= \frac{1}{\sqrt{5}}G_0 - \frac{1}{\sqrt{14}}G_2 - \sqrt{\frac{8}{35}}G_4 \\ F_{00}^2 &= \frac{1}{\sqrt{5}}G_0 - \sqrt{\frac{2}{7}}G_2 + \sqrt{\frac{18}{35}}G_4, \end{aligned} \tag{34}$$

where G_0, G_2, and G_4 are the ℓS coupling amplitudes for $\ell = 0, 2, 4$ respectively. The G_ℓ's can be calculated by solving the matrix equation

$$\begin{pmatrix} \frac{1}{\sqrt{5}} & \sqrt{\frac{2}{7}} & \frac{1}{\sqrt{70}} \\ \frac{1}{\sqrt{5}} & -\frac{1}{\sqrt{14}} & -\sqrt{\frac{8}{35}} \\ \frac{1}{\sqrt{5}} & -\sqrt{\frac{2}{7}} & \sqrt{\frac{18}{35}} \end{pmatrix} \begin{pmatrix} G_0 \\ G_2 \\ G_4 \end{pmatrix} = \begin{pmatrix} F_{20}^2 \\ F_{10}^2 \\ F_{00}^2 \end{pmatrix}. \tag{35}$$

Solving for G's, we get explicitly:

$$\begin{aligned} G_0 &= \frac{1}{3\sqrt{5}M_{f_2}^2}\cos\beta_t [g_c^{PT}(2E_{f_2}^2 + 6E_{f_2}M_{f_2} + 7M_{f_2}^2) \\ &\quad + g_d^{PT}M_{f_2}M_{\pi_2}(6E_{f_2}^2 + 18E_{f_2}M_{f_2} + 6M_{f_2}^2)] \end{aligned} \tag{36}$$

$$\begin{aligned} G_2 &= -\frac{1}{3M_{f_2}^2}\sqrt{\frac{2}{7}}\cos\beta_t [g_c^{PT}(2E_{f_2}^2 + 3E_{f_2}M_{f_2} - 5M_{f_2}^2) \\ &\quad + g_d^{PT}M_{f_2}M_{\pi_2}(3E_{f_2}^2 - 6E_{f_2}M_{f_2} + 3M_{f_2}^2)] \end{aligned} \tag{37}$$

$$\begin{aligned} G_4 &= \frac{2}{M_{f_2}^2}\sqrt{\frac{2}{35}}\cos\beta_t [g_c^{PT}(E_{f_2}^2 - 2E_{f_2}M_{f_2} + M_{f_2}^2) \\ &\quad - g_d^{PT}M_{\pi_2}M_{f_2}(2E_{f_2}^2 - 4E_{f_2}M_{f_2} + 2M_{f_2}^2)]. \end{aligned} \tag{38}$$

The D/S–ratio can be used to estimate the ratio (g_d^{PT}/g_c^{PT}) of the coupling constants. We find that, in the absence of nonlocal interactions, $G_2/G_0 = -0.018$, which is an order of magnitude smaller than the experimentally extracted value. Thus, nonlocal interactions become essential to explain the D/S–ratio for this decay. For the D/S–ratio to be equal to the value mentioned in the PDG, the ratio of the coupling constants must be $g_d^{PT}/g_c^{PT} = -0.209\ \mathrm{GeV}^{-2}$. This ratio is also of the same order of magnitude as $1/M_{\pi_2}^2$.

Finally, the decay width is given by

$$\begin{aligned} \Gamma_{\pi_2 \to f_2\pi} &= f_{\pi_2 f_2 \pi}\frac{k\cos^2\beta_t}{40\pi M_{\pi_2}^2}\left[(g_c^{PT})^2\left(\frac{4k^4}{9M_{f_2}^4} + \frac{10k^2}{3M_{f_2}^2} + 5\right)\right. \\ &\quad + 2(g_d^{PT})^2 M_{\pi_2}^2 M_{f_2}^2\left(\frac{k^4}{M_{f_2}^4} + \frac{10k^2}{M_{f_2}^2} + 10\right) \\ &\quad \left. + \frac{20}{3}g_c^{PT}g_d^{PT}E_{f_2}M_{\pi_2}\left(\frac{k^2}{M_{f_2}^2} + 3\right)\right], \end{aligned} \tag{39}$$

where $f_{\pi_2 f_2 \pi}$ is the isospin symmetry factor. The contact and derivative interactions interfere destructively to give the above decay width, as evidenced by the fact that when $g_d^{PT} < 0$, the last term is negative.

C. The $\pi_2(1670) \to \rho\pi$ decay

The vector mode of decay is described by a dimension–4 operator that has a single derivative and generates "vector" interactions, and a dimension–6 operator that has three derivatives and gives rise to "tensor" interactions. The Lagrangian including these operators is

$$\mathcal{L} = ig_v^{PT}\langle \pi_{2,\mu\nu}\rho^{\mu}\partial^{\nu}\pi\rangle + ig_t^{PT}\langle \pi_{2,\alpha\mu\nu}\rho^{\alpha\mu}\partial^{\nu}\pi\rangle, \tag{40}$$

where g_v^{PT} and g_t^{PT} are the respective coupling constants. The amplitude for the vector decay mode is

$$\begin{aligned} i\mathcal{M} &= -g_v^{PT}\epsilon_{\mu\nu}(\vec{0}, M_J)\epsilon^{\mu *}(\vec{k_1}, \lambda)k_2^{\nu} \\ &\quad - g_t^{PT}[2k_0 \cdot k_1 \epsilon_{\mu\nu}(\vec{0}, M_J)\epsilon^{\mu *}(\vec{k_1}, \lambda)k_2^{\nu} \\ &\quad - 2k_{0,\mu}k_1^{\alpha}\epsilon_{\alpha\nu}(\vec{0}, M_J)\epsilon^{\mu *}(\vec{k_1}, \lambda)k_2^{\nu}] \end{aligned} \tag{41}$$

$$= \frac{k}{\sqrt{2}}\begin{cases} (g_v^{PT} + 2g_t^{PT}M_{\pi_2}E_{\rho}) & M_J = \lambda = \pm 1 \\ \frac{2}{\sqrt{3}}\left(\frac{E_{\rho}}{M_{\rho}}g_v^{PT} + 2g_t^{PT}M_{\pi_2}M_{\rho}\right) & M_J = \lambda = 0 \end{cases}. \tag{42}$$

The helicity amplitudes can be derived using Eq. (5) and Eq. (6) just like the previous two cases. In this case, however, the allowed values of angular momentum are $\ell = 1, 3$. The helicity amplitudes are related to the PWAs through the equations

$$F^2_{10} = \sqrt{\frac{3}{10}}G_1 + \frac{1}{\sqrt{5}}G_3 \tag{43}$$

$$F^2_{00} = \sqrt{\frac{2}{5}}G_1 - \sqrt{\frac{3}{5}}G_3. \tag{44}$$

Thus, we have two PWAs, G_1 and G_3, given by

$$G_1 = -\sqrt{\frac{1}{15}}\frac{k}{M_\rho}[g_t^{PT}M_{\pi_2}M_\rho(4M_\rho + 6E_\rho) + g_v^{PT}(2E_\rho + 3M_\rho)] \tag{45}$$

$$G_3 = \sqrt{\frac{2}{5}}\frac{k}{M_\rho}[g_t^{PT}M_{\pi_2}M_\rho(2M_\rho - 2E_\rho) + g_v^{PT}(E_\rho - M_\rho)]. \tag{46}$$

In order to reproduce the measured F/P–ratio $(-0.72 \pm 0.16$, the coupling constants must have opposite sign: $g_t^{PT}/g_c^{PT} = -0.255\ \text{GeV}^{-2}$, which is of the same order of magnitude as $1/M^2_{\pi_2}$.

The decay width is given by

$$\Gamma_{\pi_2\to\rho\pi} = f_{\pi_2\rho\pi}\frac{k}{40\pi M^2_{\pi_2}}\frac{k^2}{3}\left[(g_v^{PT})^2\left(\frac{2k^2}{M^2_\rho}+5\right) + 4(g_t^{PT})^2M^2_\rho\left(\frac{3k^2}{M^2_\rho}+5\right) + 20g_v^{PT}g_t^{PT}E_\rho M_{\pi_2}\right], \tag{47}$$

where $f_{\pi_2\rho\pi}$ is the isospin symmetry factor. Again, destructive interference between the different interaction types takes place.

D. Analysis of the PWAs

We now look at the partial wave amplitudes G_0—G_4. To study the behavior of the PWAs, we look at the $\ell = 0, 2, 4$ amplitudes mentioned in Eq. (37)—Eq. (38) and the $\ell = 1, 3$ amplitudes given in Eq. (45) and Eq. (46). Below, we rewrite these equations in terms of the Lorentz factor[3] (γ). In all these expressions, we have used the symbols M_p, and $M_{d,1}$ to denote the masses of the decaying (parent, p) state and the heavier decay product (vector/tensor meson, daughter, $d, 1$) respectively.

[3]All the figures discussed in this subsection are plotted as functions of β, which is related to γ as $\gamma = \frac{E_{d,1}}{M_{d,1}} = \frac{1}{\sqrt{1-\beta^2}}$. This is because the range of β is [0, 1], whereas that of γ is $[1, \infty)$.

$$G_0 = \frac{1}{3\sqrt{5}}[g_c(2\gamma^2 + 6\gamma + 7) + g_d M_{d,1}M_p(6\gamma^2 + 18\gamma + 6)] \tag{48}$$

$$G_2 = -\frac{1}{3}\sqrt{\frac{2}{7}}[g_c(2\gamma^2 + 3\gamma - 5) + g_d M_{d,1}M_p(3\gamma^2 - 6\gamma + 3)] \tag{49}$$

$$G_4 = 2\sqrt{\frac{2}{35}}[g_c(\gamma^2 - 2\gamma + 1) - g_d M_{d,1}M_p(2\gamma^2 - 4\gamma + 2)] \tag{50}$$

$$G_1 = -\sqrt{\frac{1}{15}}\sqrt{\gamma^2 - 1}M_{d,1}[g_v(2\gamma + 3) + g_t M_p M_{d,1}(4 + 6\gamma)] \tag{51}$$

$$G_3 = \sqrt{\frac{2}{5}}\sqrt{\gamma^2 - 1}M_{d,1}[g_v(\gamma - 1) + g_t M_p M_{d,1}(2\gamma - 2)] \tag{52}$$

These expressions are valid for the decay of any $J = 2$ state to any $J = 2$ or $J = 1$ state, irrespective of their charge conjugation quantum number or the states being ground states or excited states. For example, the $2^{--} \to 1^{+-}0^{-+}$ decays proceed with $\ell = 1, 3$, and hence, the corresponding PWAs will be given by Eq. (51) and Eq. (52). Similarly, the $2^{--} \to 2^{++}0^{-+}$ decays proceed with $\ell = 0, 2, 4$ and their amplitudes will be given by Eq. (48)–(50). The difference between these decays and the ones studied in the present work lies in the value of the coupling constants. The following observations are in order:

(1) In the absence of the derivative/tensor interactions, the PWAs depend only on the Lorentz factor.
(2) The amplitudes mentioned in Eq. (48)—Eq. (51) are plotted in Fig. 2. The plots on the top row show the contributions of the contact and derivative interactions to the PWAs as functions of β. On the bottom row are the corresponding vector and tensor contributions to the vector mode of the pseudotensor decay. All the higher partial waves (G_1, G_2, G_3, and G_4) vanish as the momentum carried by the decay products goes to zero (i.e., nonrelativistic limit). In this limit, the S–wave has the amplitude proportional to $\sqrt{5}(g_c + 2g_d M_p M_{d,1})$. We infer from Eq. (51) that the P–wave amplitude also vanishes in the nonrelativistic limit, due to an overall multiplying factor of $\sqrt{\gamma^2 - 1}$.
(3) In the ultrarelativistic limit (i.e., $\beta \to 1$), the higher partial waves dominate over the S–wave and the P–wave. In this case, the D/S, G/S, and the F/P–ratios become much larger than 1, as can be seen

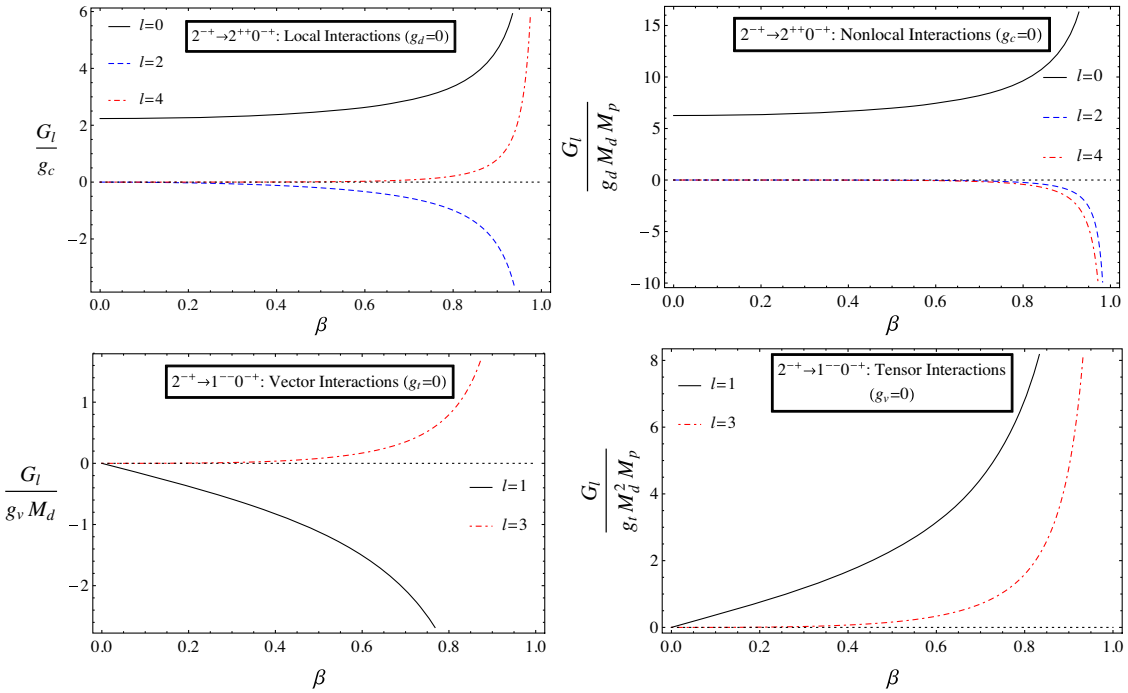

FIG. 2. Plots of the partial wave amplitudes (scaled appropriately) as functions of β: lower order terms (left), higher order terms (right); tensor decay mode (above), vector decay mode (right). See Sec (III D) for a detailed description.

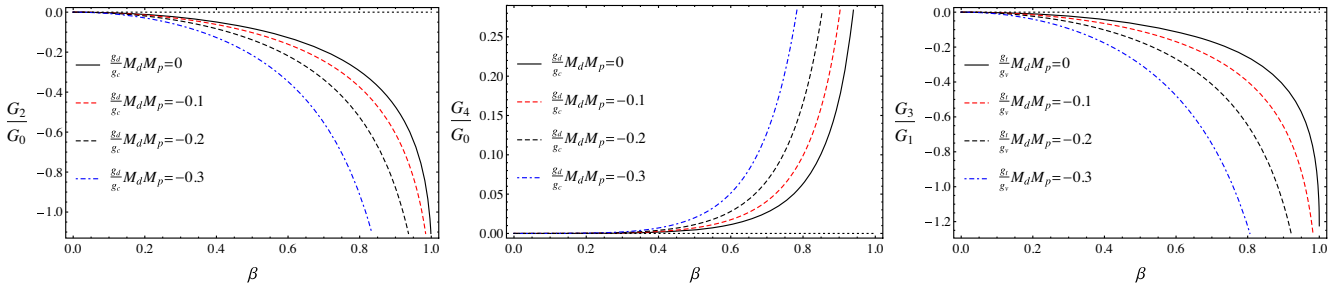

FIG. 3. The D/S–, G/S–, and the F/P–ratios (left, center, and right respectively) as functions of β for representative values of $\frac{g_d}{g_c}M_pM_{d,1}$ and $\frac{g_t}{g_v}M_pM_{d,1}$.

from Fig. 3. In the tensor mode of the decay of the pseudotensor meson, the G/S–ratio becomes larger than the D/S–ratio. The behavior of the PWAs in this region is dominated by the derivative/tensor interaction (i.e., higher order contributions to the Lagrangian).

IV. COUPLING CONSTANTS, ISOSCALAR MIXING ANGLES, AND THEIR CONSEQUENCES

In this section, we employ the formalism described in the previous section in order to evaluate PWA for various nonet members, to determine the coupling constants, the strange-nonstrange mixing angle of the isoscalar members of a given nonet, and to discuss their consequences.

A. $J^{PC}=1^{++}$

In this subsection, we demonstrate the working of our model by applying it to the $J^{PC}=1^{++}$ nonet. In this sector, the Lagrangian h as three parameters: the coupling constants g_c^A and g_d^A, and the isoscalar mixing angle[4] θ_a. The mixing angle enters the Lagrangian through the scheme

$$\begin{pmatrix} |f_1\rangle \\ |f_1'\rangle \end{pmatrix} = \begin{pmatrix} \cos\theta_a & \sin\theta_a \\ -\sin\theta_a & \cos\theta_a \end{pmatrix} \begin{pmatrix} |\bar{n}n\rangle_a \\ |\bar{s}s\rangle_a \end{pmatrix}, \quad (53)$$

[4]Here, and everywhere else, the Lagrangian describing the decays of the isoscalars is identical to that for the decays of the isovectors, except for the isospin symmetry factors.

where $|\bar{s}s\rangle_a$ and $|\bar{n}n\rangle_a (= \frac{1}{\sqrt{2}}(|\bar{u}u\rangle_a + |\bar{d}d\rangle_a))$, where the subscript "$a$" represent axial-vector states, are the strange and nonstrange isosinglet states respectively. We also have three data points: the D/S–ratio and the width of the $a_1(1260) \to \rho\pi$ decay, and the width of the $f_1'(1420) \to K^*K$ decay. The PDG lists the D/S–ratio for the $a_1(1260) \to \rho\pi$ decay as -0.062 ± 0.02 [1]. Since the $\rho\pi$ channel is the dominant channel for the decay of the $a_1(1260)$, we take the total width (420 ± 35 MeV) of the $a_1(1260)$ as the width of this channel. The width of the $f_1'(1420) \to K^*K$ decay can be estimated as 44.5 ± 4.2 MeV, using the branching fraction listed in the PDG [1]. Since the number of unknowns is the same as the number of data points available, the values of the parameters can be estimated without resorting to a statistical fit. We, however, define the χ^2 function so as to calculate the errors in the values of the parameters and those in the widths and PWA ratios. The input values are listed in Table I and the values of the parameters so obtained are listed in Table II.

We use the values of the parameters thus obtained to estimate the D/S–ratios and the widths for the kaonic decays of $f_1(1285)$ and $f_1'(1420)$. These values are listed in Table III. Of these two decays, the $f_1(1285) \to K^*K$ is decay is sub-threshold and hence kinematically suppressed. We perform a spectral integration over the final K^* to obtain the width and the D/S–ratio for this decay (see Appendix A for details). We make the following observations:

(1) The small value of the D/S–ratio for the 1^{++} decays indicate that the D–wave interactions, which are predominantly derivative interactions, play only a minor role. Correspondingly, the coupling constant g_d^A has a small value (compatible with zero). In other words, $g_c^a/g_d^A \ll M_{a_1}^2$.

(2) The mixing of the isoscalars is an important feature of QCD. The value of the 1^{++} isoscalar mixing angle obtained in the present work ($\theta_a = (24.9 \pm 3.2)^\circ$) is consistent with the experimental value ($\pm(24.0^{+3.7}_{-3.4})^\circ$) reported in [45] as well as the lattice results ($(31 \pm 2)^\circ$) [46] (see also Refs. [47,48] for comparison). The isosinglet mixing angles in the $J = 1$ sector are sensitive to the masses and mixing angle of the corresponding kaons, if viewed through the Gell-Mann-Okubo (GMO) mass relations. However, the $\bar{B}^0 \to J/\psi f_1(1285)$ and the $\bar{B}_s^0 \to J/\psi f_1(1285)$ decays provide a much cleaner view into the mixing between $f_1(1285)$ and $f_1'(1420)$. The ratio of the branching fractions of these two decays is proportional to $\tan^2\theta_a$ and, more importantly, independent of the kaonic mixing angle [45,49]. However, we note that, this measurement cannot give us the information regarding the sign of the mixing angle.

(3) We compare the values of the D/S–ratios we obtain with those extracted using the $^3P_0$ model [33]. A brief review of the $^3P_0$ model is presented in Appendix B and the corresponding results are listed in Table XIV. We see that, for the $a_1(1260) \to \rho\pi$ decay, our value agrees with PDG average [1], where as the $^3P_0$ values are compatible with the values obtained by the E852 [42], OPAL [43], and the ARGUS [44] collaborations. Our value is nearly 2.5 times smaller than the $^3P_0$ one. This carries over to the decay of the isoscalar meson as well. Our estimate for the D/S–ratio of the $f_1'(1420) \to K^*K$ decay is nearly 3.5 times smaller than that from the $^3P_0$ model.

TABLE I. Input values used to extract the values listed in Table II.

Decay	Width (MeV)	D/S [1]
$a_1(1260) \to \rho\pi$	420 ± 35	-0.062 ± 0.02
$f_1'(1420) \to K^*K$	44.5 ± 4.5	$---$

TABLE II. Values of the parameters used in the decays of the axial-vector mesons.

g_c^A (GeV)	g_d^A (GeV^{-1})	θ_a
3.89 ± 0.75	-0.32 ± 0.37	$(24.9 \pm 3.2)^\circ$

TABLE III. Predictions based on the parameters listed in Table II. See text for details of the calculations.

Wdith (MeV)		
Decay	Theory	PDG [1]
$f_1(1285) \to K^*K$	4.78 ± 0.57	not seen
D/S–ratio		
Decay	Theory	PDG [1]
$f_1(1285) \to K^*K$	$-(0.436 \pm 0.87) \times 10^{-3}$	$---$
$f_1'(1420) \to K^*K$	-0.0116 ± 0.005	$---$

B. $J^{PC} = 1^{+-}$

We now turn our attention to the decays of the pseudovector mesons. The Lagrangian describing the $1^{+-} \to 1^{--}0^{-+}$ decays is similar to the one written in Eq. (21). Thus, we have three parameters: the coupling constants g_c^B and g_d^B, and the isoscalar mixing angle θ_{pv}. Similar to the case of axial-vectors, the mixing angle is defined through the relation

$$\begin{pmatrix} |h_1\rangle \\ |h_1'\rangle \end{pmatrix} = \begin{pmatrix} \cos\theta_{pv} & \sin\theta_{pv} \\ -\sin\theta_{pv} & \cos\theta_{pv} \end{pmatrix} \begin{pmatrix} |\bar{n}n\rangle_{pv} \\ |\bar{s}s\rangle_{pv} \end{pmatrix}, \quad (54)$$

TABLE IV. Input values used to extract the values listed in Table V.

Decay	Width (MeV)	D/S [1]
$b_1(1235) \to \omega\pi$	110 ± 7[17]	0.277 ± 0.027
$h_1'(1415) \to K^*K$	90 ± 15[1]	$---$

TABLE V. Values of the parameters used in the decays of the pseudovector mesons.

g_c^B (GeV)	g_d^B (GeV^{-1})	θ_{pv}
6.36 ± 0.72	-4.37 ± 0.37	$(25.2 \pm 3.1)^\circ$

where the subscript pv implies psuedovector. The values of these three parameters can be obtained using the width and D/S–ratio of the $b_1(1235) \to \omega\pi$ decay, and the width of the $h_1'(1415) \to K^*K$ decay. The values of the input parameters are listed in Table IV. We note that, the PDG does not list the partial widths of the decays of the 1^{+-} mesons. Hence, we have used the values obtained in an earlier work [17] for the width of the $b_1(1235) \to \omega\pi$ decay, and the total width of the $h_1'(1415)$ as the width of the $h_1'(1415) \to K^*K$ decay, as this is the only observed channel [1]. The values of the parameters obtained using these data and the associated errors are listed in Table V.

(1) In the decays of the pseudovector mesons, the D–waves interfere largely constructively with the S–waves. It should be noted that there exists a small phase difference of $(10 \pm 5)^\circ$ between the D–wave and the S–wave in the $b_1(1235) \to \omega\pi$ decay [1]. However, we have not been able to reproduce this phase difference. Further, in the absence of the derivative interactions, the D/S–ratio of the $b_1(1235) \to \omega\pi$ decay is negative and is nearly equal to the corresponding ratio for the $a_1(1260) \to \rho\pi$ decay. The nonlocal interactions introduced in the form of the dimension–5 operators contribute a large amount to the D/S–ratio to make it significantly large and positive. This signifies that the nonlocal interactions play a crucial role in the pseudovector sector.

(2) The values of the parameters listed in Table V are significantly different from the values derived in Ref. [17]. This can be attributed to two reasons: the introduction of the derivative interactions in the pseudovector sector, and the mixing of the isosinglet states. Derivative interactions were used to analyze the decay of $b_1(1235)$ in [29]. The coupling constants g_1 and g_2 mentioned there have been rendered dimensionless by the multiplying/dividing mass term. The ratio of the two coupling constants used in our work, g_d^B/g_c^B matches the corresponding value from Ref. [29],[5] as can be seen from Table II. The absolute values of the coupling constants are slightly different as we have included the isosinglet states as well in our work as opposed to only the isotriplet in [29]. However, as far as the D/S–ratio is concerned, only the ratio of the coupling constants matters. Further, we have taken the partial decay width for the $b_1(1235) \to \omega\pi$ decay as 110 ± 7 MeV, instead of the full width of 142 ± 9 MeV.

(3) The value of the coupling constant g_c^B is nearly twice that of g_c^A, as shown in Table II. This is particularly interesting, as the pseudovector states differ from the axial-vector states only in the charge conjugation, the decay products belong to the same set of nonets, and the 3-momenta carried by the decay products in both the cases are nearly the same.

(4) We also note that, in general, the influence of the D–wave on the decay of the mesons reduces as the 3-momenta of the decay products decreases, as seen by the decreasing values of the D/S–ratio. This is a feature we observe irrespective of the spin of the decaying state. This indicates that, when a meson decays into a closely lying state (specifically, if the associated 3-momentum is small) the angular distribution of the decay products is mostly spherical, and one may not lose much information if the higher partial waves are not included while analyzing the experimental data.

(5) The mixing angle between the pseudovector isoscalars comes out to be larger than the value extracted by the BESIII collaboration [50]. Our estimate of the mixing angle is $(25.2 \pm 3.1)^\circ$, where as the BESIII collaboration reports a nearly zero mixing among the strange and nonstrange states ($\theta_{pv} = (0.6 \pm 2.6)^\circ$), which agrees with the lattice results ($(3 \pm 1)^\circ$) [46]. One should however note that, the analysis of the BESIII is based on the mass of the $h_1(1415)$ and is very much sensitive to the value of the kaonic mixing angle which, in turn, is based on the GMO mass relations [51]. Thus, a better avenue, similar to the case of the axial-vector, is needed to get a good insight into the mixing of pseudovector isosinglets. According to our analysis, a significantly large mixing angle is necessary to explain the smaller width of $h_1(1415)$. With the mixing angle we obtain, the $h_1(1415)$ can be seen as a mixture of approximately 83% $|\bar{s}s\rangle$ and 17% $|\bar{n}n\rangle$ and vice versa for the $h_1(1170)$.

(6) The parameters obtained have been used to calculate the D/S–ratio and the width of the $h_1(1170) \to \rho\pi$ decay as well as the D/S–ratio of the $h_1'(1415) \to K^*K$ decay. These values are listed in Table VI. We

[5]We point out a misprint in [29], i.e., the value of g_1 must be -8.37 instead of the -1.34 given in the article.

TABLE VI. Predictions based on the parameters listed in Table V. See text for details of the calculations.

Width (MeV)		
Decay	Theory	PDG [1]
$h_1(1170) \to \rho\pi$	146 ± 14	seen
D/S–ratio		
Decay	Theory	PDG [1]
$h_1(1170) \to \rho\pi$	0.281 ± 0.035	− − −
$h_1'(1415) \to K^*K$	0.021 ± 0.001	− − −

observe that the D/S–ratio for the $h_1(1170) \to \rho\pi$ decay is marginally higher than that for the $b_1(1235) \to \omega\pi$ decay even though the $\omega\pi$ carry significantly larger 3-momentum (348 MeV) than the $\rho\pi$ (303 MeV). This is because, the S–wave amplitude in the $b_1(1235) \to \omega\pi$ decay is nearly 36% higher than that of the $h_1(1170)\rho\pi$ decay whereas the D–wave amplitude is only ∼33% larger.

(7) We compare our estimates of the D/S–ratios of the decays of the pseudovector mesons with those obtained from the $^3P_0$ model. Unlike the values for the decays of the axial-vector mesons, our values are nearly in good agreement with those from the $^3P_0$ model (see Appendix B and the Table XIV therein).

C. $J^{PC} = 2^{-+}$

We now turn our attention to the decay of the 2^{-+} mesons. Here, we have analyzed two kinds of decays: $2^{-+} \to 2^{++}0^{-+}$ (tensor mode) and $2^{-+} \to 1^{--}0^{-+}$ (vector mode). The tensor decay mode is described by the Lagrangian given in Eq. (31) and the vector mode by Eq. (40). Each of the Lagrangians contain two parameters: the tensor mode coupling constants g_c^{PT} and g_d^{PT}, and the vector mode coupling constants g_v^{PT} and g_t^{PT}, the values of which are listed in Table VII. The data used as inputs to derive the values of these parameters are listed in Table VIII. The decay widths listed in Table VIII have been calculated using the branching fractions listed in the PDG [1]. The values of the parameters can be estimated similar to the case of the $J^P = 1^+$ nonets. Using these parameters, we calculate the ratios of the PWAs and the widths for the $\pi_2(1670) \to f_2'(1520)\pi$, and $\pi_2(1670) \to K^*K$ decays. These values are listed in Table IX. We make the following observations:

TABLE VII. Values of the parameters used in the decays of the pseudotensor mesons.

g_c^{PT} (GeV)	g_d^{PT} (GeV^{-1})	g_v^{PT}	g_t^{PT} (GeV^{-2})
39 ± 13	-8.16 ± 2.95	-9.44 ± 1.24	2.41 ± 0.50

TABLE VIII. Input values used to extract the values listed in Table VII.

Decay	Width (MeV)	D/S [1]	F/P [1]
$\pi_2(1670) \to f_2(1270)\pi$	146.4 ± 9.7	-0.18 ± 0.06	× × ×
$\pi_2(1670) \to \rho\pi$	80.6 ± 10.8	× × ×	-0.72 ± 0.16

(1) In the absence of derivative interactions, the D/S–ratio for the $\pi_2(1670) \to f_2(1270)\pi$ decay is an order of magnitude smaller than the experimentally extracted value. In the case of the $\pi_2(1670) \to \rho\pi$ decay, in the absence of the tensor interactions, the value of the F/P–ratio comes out to be less than 1/5th of the experimental value. Thus, the nonlocal/tensor interactions contribute to a large extent to the decay of the tensor mesons. A closer inspection of the amplitudes of the individual partial waves [Eq. (37)–(38)] show that the coupling constant for the derivative interactions decides the sign of each amplitude in case of the tensor decay mode.

(2) According to our analysis, the contributions of the $\ell = 4$ wave to the decay of tensor mesons is nearly two orders of magnitude smaller than the $\ell = 2$ waves. But, the D–waves and the G–waves interfere destructively. Here again, the nonlocal interactions play an important role in deciding the phases of these waves relative to the S–wave.

(3) The $J = 2$ isosinglets pose a special problem. The nature of $\eta_2(1870)$ is still a mystery. The absence of evidence for the K^*K decay mode makes it difficult to interpret it as the heavier sibling of the $\eta_2(1645)$ [14,52]. Without this state, though, the 2^{-+} nonet is incomplete. Further, the angle of mixing between the two isosinglet is still an open problem. The mixing angle (β_{pt}), given by the scheme

$$\begin{pmatrix} |\eta_2\rangle \\ |\eta_2'\rangle \end{pmatrix} = \begin{pmatrix} \cos\beta_{pt} & \sin\beta_{pt} \\ -\sin\beta_{pt} & \cos\beta_{pt} \end{pmatrix} \begin{pmatrix} |\bar{n}n\rangle_{pt} \\ |\bar{s}s\rangle_{pt} \end{pmatrix} \quad (55)$$

where pt stands for pseudotensor, is expected to be large in this sector as the 2^{-+} mesons are heterochiral states [30]. A recent work [53] reported that the mixing angle for the $\eta_2(1645)$ and $\eta_2(1870)$ to has to be larger than the value (14.8°) derived using the GMO relations to properly fit the decay widths. The value of the mixing angle was found to be −42°[53]. However, this failed to reproduce the ratio of branching fractions of the decays $\eta_2(1870) \to a_2\pi$ to $\eta_2(1870) \to f_2\eta$. The value of this ratio calculated in Ref. [53] was 23.5, which is an order larger than the value 1.7 ± 0.4 accepted by PDG [1] (but, close to the value extracted by the WA102 collaboration [54]). For the present analysis, we proceed assuming that the $\eta_2(1870)$ is the isosinglet of the pseudotensor nonet. The Lagrangian that

TABLE IX. Predictions based on the parameters listed in Table VII. See text for details of the calculations.

Decay	Width (MeV)	D/S	G/S	F/P
$\pi_2(1670) \to f_2(1270)\pi$	*Input*	*Input*	0.0042 ± 0.0014	$\times\times\times$
$\pi_2(1670) \to f_2'(1520)\pi$	0.43 ± 0.21	0.00925 ± 0.0031	$-(7.49 \pm 2.7) \times 10^{-6}$	$\times\times\times$
$\pi_2(1670) \to K^*K$	5.11 ± 1.4	$\times\times\times$	$\times\times\times$	-0.447 ± 0.099

describes the decays of these isoscalars are similar to the ones given in Eq. (31) and Eq. (40), except for the mixing and the isospin factors. In Fig. 4, we have plotted the ratio of the widths of the $\eta_2(1645) \to a_2(1320)\pi$ and $\eta_2(1645) \to K^*K$ decays as functions of the mixing angle. The dashed horizontal line in the Fig. 4 represents the experimental value of this ratio (0.07 ± 0.03) [1,55]. We see that two values of mixing angle can reproduce this data: $\beta_{pt} = -(44.2^{+11}_{-15})^\circ$ and $+(67.3^{+2.5}_{-4.1})^\circ$. The uncertainties in the allowed values of β_{pt} arise from the uncertainties in the experimental data. Calculating the widths of these decays of the $\eta_2(1645)$ will allow us to narrow down the value of the mixing angle further. The values of the decay widths, given in Table X, show that the positive mixing angle underestimates the width of the $\eta_2(1645)$ by nearly a factor of 3.5. Assuming that the $a_2\pi$ channel is the dominant channel for the decay of the $\eta_2(1645)$, the sum of its width along with that of the K^*K channel must be close to the total width of the $\eta_2(1645)$. This sum comes out be $\approx 198 \pm 15$ MeV for the negative mixing angle and $\approx 58 \pm 5$ MeV for the positive angle. These observations hint that the isoscalar mixing angle in the 2^{-+} sector must be negative and close to 45°, consistent with the earlier study reported in Ref. [53].

(4) The ratios of the PWAs for the above discussed decays of the $\eta_2(1645)$ are listed in Table XI. These ratios are independent of the mixing angle. It can be seen from the table that the ratios of PWAs have the same behavior as of those for the decays of the $\pi_2(1670)$. The D–waves are less pronounced in the decay of the $\eta_2(1645)$ to the $a_2\pi$ compared to the case of $\pi_2(1670) \to f_2\pi$ as the $\eta_2(1645)$ is marginally lighter than its isovector sibling and the decay product is slightly heavier than $f_2(1270)$ resulting in the 3-momentum carried by the $a_2\pi$ being smaller. But, in the vector mode of the decay, the F/P–ratio is comparable to that of the $\pi_2(1670) \to K^*K$, as the 3-momenta are nearly the same.

(5) We plot the ratio of the widths of the $\eta_2(1870) \to a_2(1320)\pi$ and $\eta_2(1870) \to f_2(1270)\eta$ decays in the Fig. 5. The value of this ratio was reported as 1.7 ± 0.4 in the PDG [1]. From the Fig. 5, we see that, for this ratio to be small, the mixing angle must be close to zero. It should be noted that, a conventional $\bar{q}q$ model of the $\eta_2(1870)$ predicts the $a_2\pi$, $f_2\eta$, and the K^*K channels to be dominant and the mixing angle to be close to zero [56].

(6) As shown in the Fig. 5, the local and nonlocal interactions taken separately contribute nearly identically. However, when combined, the width of the $f_2(1270)\eta$ channel (which appears in the denominator) becomes very small leading to a large ratio except when the mixing angle is very small. When the mixing angle takes the values mentioned in point 3 above, the decay widths of the three channels of $\eta_2(1870)$ become significantly smaller than its total width. Specifically, the width of the $f_2(1270)\eta$

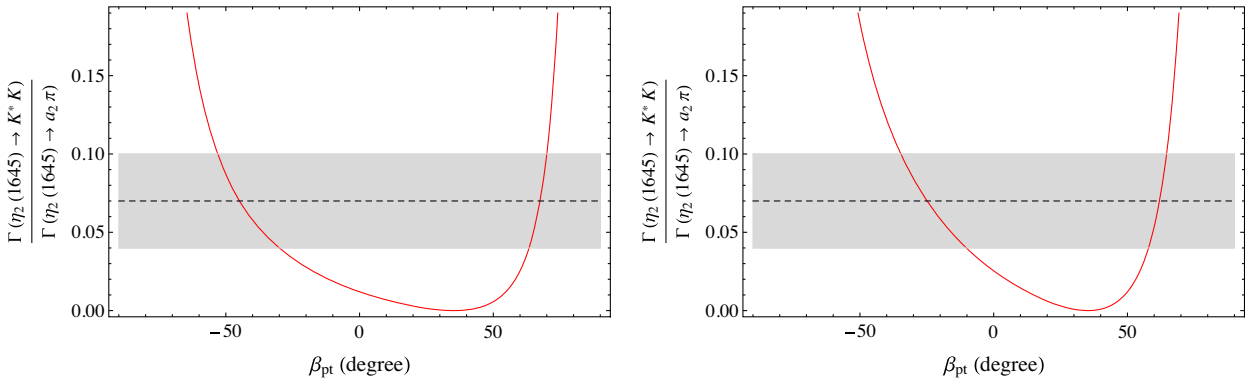

FIG. 4. Plot of ratio of the partial widths of the two modes of decays of $\eta_2(1645)$ discussed in the text, as a function of the mixing angle: (left) including higher order terms and (right) without the higher order terms. The shaded region represents the uncertainty in the experimental value.

TABLE X. Widths of the of decays of $\eta_2(1645)$ and $\eta_2(1870)$ studied in this work. The uncertainties are from the uncertainties in the coupling constants. The uncertainties in the mixing angle have not been considered.

	Width (MeV)	
Decay	$\beta_{pt} = -(44.2^{+11}_{-15})^\circ$	$\beta_{pt} + (67.3^{+2.5}_{-4.1})^\circ$
$\eta_2(1645) \to a_2\pi$	185 ± 12	54.1 ± 3.6
$\eta_2(1645) \to K^*K$	12.9 ± 3.28	3.78 ± 0.95
$\eta_2(1870) \to a_2\pi$	50.7 ± 9.2	87 ± 23
$\eta_2(1870) \to f_2(1270)\eta$	0.16 ± 0.84	0.56 ± 2.1
$\eta_2(1870) \to K^*K$	0.65 ± 0.15	15.8 ± 3.2

channel becomes very close to zero (see Table X). On the other hand, if the mixing angle is taken to be small and nonzero ($\beta_{pt} = -1.17^\circ$ or $\beta_{pt} = 1.42^\circ$), then the width of the $\eta_2(1645) \to a_2\pi$ decay is approximately 368 MeV, which is nearly twice the total width of the $\eta_2(1645)$. Thus, it appears from our analysis that the heavier sibling of the $\eta_2(1645)$ cannot have a mass close to the mass of the $\eta_2(1870)$. This indicates that the $\eta_2(1870)$ is not a member of the 2^{-+} $\bar{q}q$-nonet, consistent with the earlier analyses [10,33,52,57].

(7) Finally, we compare our results with the results from the $^3P_0$ model (Table XIV). We observe that according to the $^3P_0$ model, all the allowed partial waves (i.e., the S–, D–, and the G–waves) interfere constructively in the tensor mode of the decay of the 2^{-+} mesons. However, this is in contrast with the experimental observations, where, the D–waves interfere destructively with the S–waves as indicated by the negative D/S–ratio. Unfortunately, no information is available about the nature of the G–waves. But for this difference in the sign of the ratios, we find that our value for the $\pi_2(1670) \to f_2(1270)\pi$ decay agrees very well with that from the $^3P_0$ model. However, for the other two decays we observe large deviations (factors of 1.5 and 4) from the values of the $^3P_0$ model. In the vector decay mode, our values agree fairly well with those of the $^3P_0$ model, assuming similar errors in both the sets of values.

D. Effects of form factors

The virtual cloud of quarks and antiquarks surrounding the constituent quarks and/or antiquarks enhance their masses and contribute significantly to the charge radii of the hadrons and hence give rise to finite sizes of hadrons [58,59]. The nonpointlike nature of the mesons brings forth the question of whether a tree-level analysis captures the physics of their decays effectively. In the absence of a fundamental theory or a systematic effective theory, we are forced to use empirical form factors to include the finite-size effects on the decays. Various types of form factors have been used in the past to model the structure of the mesons including, but not limited to Gaussian, exponential, multipole, etc. Specifically, the Gaussian form factors have been used in nonrelativistic quark models to study the decays and interactions of mesons [33,60], the interactions between the nucleons [61,62] as well as in field theoretic models to study line shapes of various mesons [63]. We make use of the Gaussian form factor of the form [33,60]

$$F(k,\beta) = e^{-\frac{k^2}{12\beta^2}}. \tag{56}$$

The form factor contributes to the decay width in the form

$$\Gamma_F = \Gamma |F(k,\beta)|^2, \tag{57}$$

where Γ_F and Γ are the decay widths with and without form factors respectively. This is based on the assumption that the decay amplitudes ($i\mathcal{M}$) must be modified to $i\mathcal{M}F(k,\beta)$. Thus, the ratios of PWAs are unaffected by the inclusion the form factor. The typical value of β used in the quark model calculations (e.g., the $^3P_0$ model) is 0.4–0.5 GeV [60]. In the present work, we use the value $\beta = 0.4$ GeV. We then extract the values of the parameters using the procedure described in the previous subsections. The values of these parameters are listed in Table XII. Since the value of the form factor for nonzero 3-momentum is always less than one, the parameters become slightly larger when form factor is included. However, the new values and the old values overlap significantly. Thus, even though the form factor modifies the decay widths, the change is not drastically large.

The need to include nonlocal/tensor interactions to explain the properties of the mesons discussed in this paper tells us that the internal dynamics of the mesons play a crucial role in their decays. Naively speaking, the need for the higher dimension operators indicate the possibility of a scale associated with these processes. Along these lines we would like to note that, the magnitude of the ratios of the parameters g_v^{PT}/g_t^{PT} is approximately 3.92 GeV^2 ($\sim 1.5 M_{\pi_2}^2$) for the pseudotensor coupling constants. For the tensor modes, the ratio $|g_c^{PT}/g_d^{PT}|$ is 4.78 GeV^2 ($\sim 2M_{\pi_2}^2$) for

TABLE XI. The ratios of the PWAs for the decays of $\eta_2(1645)$ discussed in the text.

Decay	D/S	G/S	F/P
$\eta_2(1645) \to a_2(1320)\pi$	-0.089 ± 0.029	0.0011 ± 0.0004	$--$
$\eta_2(1645) \to K^*K$	$--$	$--$	-0.32 ± 0.07

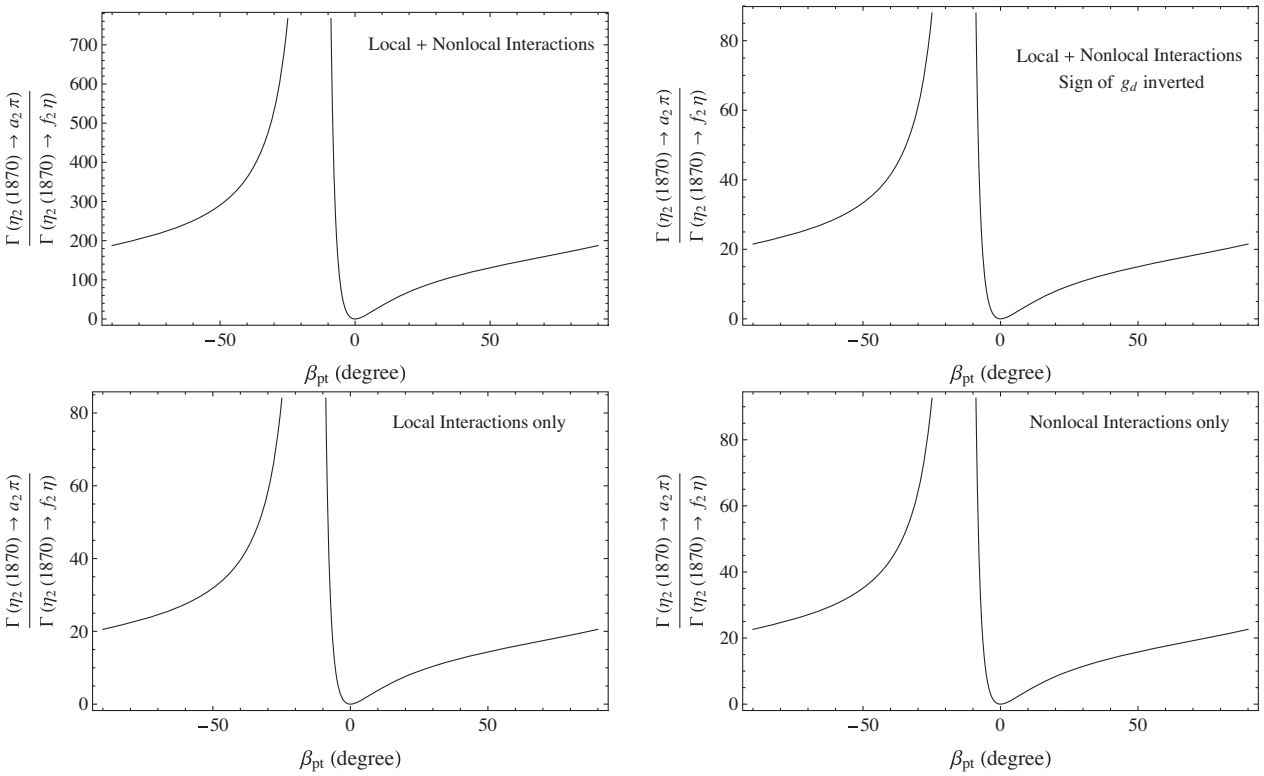

FIG. 5. Plot of the ratio partial widths of the two modes of decays of $\eta_2(1870)$ discussed in the text: (above, left) as a function of mixing angle; (above, right) with the sign of the coupling constant for derivative interaction flipped; (below) contributions of the local (left) and nonlocal interactions (right) as a function of mixing angle.

pseudotensor coupling constants. Similarly, the corresponding ratio in the pseudovector sector is $|g_c^B/g_d^B|$ is approximately 1.52 GeV^{-2} ($\sim M_{b_1}^2$). From these, we deduce that, for the pseudotensors $g_v^{PT} \sim M_{PT}^2 g_t^{PT}$, $g_c^{PT} \sim M_{PT}^2 g_d^{PT}$, and $g_c^B \sim M_B^2 g_d^B$ for the pseudovectors, implying that nonlocal interactions play an important a role.

V. SUMMARY AND OUTLOOK

In this work, we have studied the vector decays of the axial-vector, pseudovector, and pseudotensor mesons, and the tensor decays of the pseudotensor mesons. We have derived the partial wave amplitudes for these decays using the covariant helicity formalism. We have demonstrated that the nonlocal interactions play a crucial role in these decays, except in the decays of the axial-vector mesons, where, contact interactions can reproduce the decay widths and the ratio of the PWAs up to a reasonable accuracy. The partial decay widths can be reproduced within the limits of experimental errors and theoretical uncertainties using our approach.

We also have estimated the mixing angle between the isosinglets in the $J = 1$ sector. The angle of mixing between the axial-vector isosinglets agrees with the experimentally derived value. But, our model disagrees with the experiments in the pseudovector sector.

Similarly, in the decays of the pseudotensor isovectors, the derivative/tensor interactions play a major role and are essential to describe the ratios of the PWAs. We have also studied the isoscalar mixing and we find that the mixing angle must be large and negative ($\approx -44°$). Further, we find that the interpretation of the $\eta_2(1870)$ as the heavier partner of the $\eta_2(1645)$ needs further studies. More information about the η_2 states, in the form of the values of the branching ratios, can help us pin down the mixing angle as well as the nature of the $\eta_2(1870)$.

As reported in [64], the decay of the $\pi_1(1600)$ into $b_1(1235)\pi$ is know to receive a significant contribution from the D–waves. A study along these lines can help in revealing the nature of the hybrid. Also of interest are the $J = 1$, 2 kaons, which are known to exhibit internonet mixing. Investigation of the partial waves of the kaonic decay can possibly settle the debate on the angle of mixing between these states [65].

Moreover, in the future one can extend the present study in various directions, e.g., to higher spin as $J = 3$ [66,67], where the results can be compared to the lattice results [68], and to baryonic decays. Quite interestingly, the study of PWA is not confined to the strong interaction only. Another important future works include the link of PWA to loop effects, thus going beyond tree-level studied in this work. This can be achieved by taking into account the widths of the unstable states, both in the initial and the final states.

TABLE XII. Values of the parameters when form factor is included.

g_c^A (GeV)	g_d^A (GeV^{-1})	θ_a	g_c^B (GeV)	g_d^B (GeV^{-1})	θ_{pv}
4.08 ± 0.79	-0.34 ± 0.39	$(26.1 \pm 3.0)^\circ$	6.67 ± 0.75	-4.58 ± 0.38	$(26.5 \pm 3.0)^\circ$
g_c^{PT} (GeV)	g_d^{PT} (GeV^{-1})	g_v^{PT}	g_t^{PT} (GeV^{-2})		
41 ± 13	-8.51 ± 3.10	-11.1 ± 1.46	2.83 ± 0.59		

In conclusion, partial wave analysis of the decay processes can provide deeper insights into the structure and properties of conventional mesons as well as exotic states and can be of great use in future studies of resonances.

ACKNOWLEDGMENTS

We are thankful to U. Raha and A. Koenigstein for useful discussions. F. G. and V. S. acknowledge financial support through the Polish National Science Centre (NCN) via the OPUS Project No. 2019/33/B/ST2/00613. F. G. acknowledges also support from the NCN OPUS Project No. 2018/29/B/ST2/02576. E. T. acknowledges financial support through the project AKCELERATOR ROZWOJU Uniwersytetu Jana Kochanowskiego w Kielcach (Development Accelerator of the Jan Kochanowski University of Kielce), co-financed by the European Union under the European Social Fund, with No. POWR.03.05.00-00-Z212/18.

APPENDIX A: UNSTABLE STATES IN DECAY PRODUCTS

Some of the decays discussed in this paper involve unstable final states, e.g., $a_1(1260) \to \rho\pi$, $h_1(1170) \to \rho\pi$, and $\pi_2(1670) \to \rho\pi$. Modeling these decays using only the tree level diagrams, *prima facie*, does not capture the complete dynamics of the decay process. The instability of the final state can be taken into account by integrating the decay width weighted by the spectral function of the unstable state. Accordingly, for the decay process $A \to BC$ with B unstable, the actual decay width can be written as

$$\Gamma_T = \int_{s_{th}}^{\infty} ds \Gamma_{\text{tree}}(s) d_B(s), \tag{A1}$$

where $d_B(s)$ is the spectral function of B, $\sqrt{s} = M_B$, and s_{th} is the threshold for the decay of B. In spite of this apparent shortcoming, we find that the decay widths do not vary significantly from their tree-level values, as we show using the three decays mentioned earlier.

Typically, the Breit-Wigner form of the spectral function is used to model the unstable state. In this work, we use a different parametrization of the spectral function, called the Sill distribution, which, is normalized to unity and has a built-in threshold [69]. In all the example decays, the final unstable states is the ρ–meson which decays primarily into two pions. Thus, it is sufficient if we use the single channel Sill distribution. The explicit form of distribution function is [69]

$$d_{B=\rho}(s) = \frac{1}{\pi} \frac{\tilde{\Gamma}\sqrt{s - s_{th}}}{(s - m_\rho^2)^2 + (\tilde{\Gamma}\sqrt{s - s_{th}})^2}, \tag{A2}$$

where $\tilde{\Gamma} = \frac{\Gamma_\rho m_\rho}{\sqrt{m_\rho^2 - s_{th}}}$, m_ρ is the mass of the ρ–meson and Γ_ρ is its total width. The decay width mentioned in the integrand of Eq. (A1) is given by the Eq. (30) and Eq. (47) with the mass $M_\rho = \sqrt{s}$. We list the decay widths obtained in the Table XIII. The errors listed are based on the assumption that the fractional errors before and after spectral integration are the same. The widths of the decays do not vary greatly after spectral integration.

APPENDIX B: COMPARISON WITH THE $^3P_0$ MODEL

In this Appendix, we compare our results with those obtained using the $^3P_0$ model. Before presenting the results, we briefly describe the $^3P_0$ model, and list the PWAs given in [33].

The $^3P_0$ model is essentially a flux-tube breaking model. In this model, the mesons are assumed to have quark-antiquark pairs with chromoelectric or chromomagnetic flux lines between them. The strong decays of these mesons occur when these flux tubes break and create a quark-antiquark pair. The two quarks and two antiquarks then rearrange into two quark-antiquark pairs which are interpreted as two mesons [70]. The Hamiltonian for such a decay is based on the Hamiltonian of the lattice QCD and is given by:

$$\hat{H}|\vec{r}_1, \vec{r}_2\rangle = \gamma F(\vec{r}, \vec{w}) \Psi^\dagger(\vec{R}) \vec{\alpha} \cdot \overleftrightarrow{\nabla} \Psi(\vec{R}) |\vec{r}_1, \vec{r}_2\rangle, \tag{B1}$$

where $\Psi(\vec{R})$ is the wave function of the $\bar{q}q$ pair created at position $\vec{R}$ with (quark model) quantum numbers $^3P_0$, γ is a

TABLE XIII. Comparison of the tree-level widths of the three decays with the integrated widths.

Decay	Tree-level width (MeV)	Integrated width (MeV)
$a_1(1260) \to \rho\pi$	420 ± 35	354 ± 30
$h_1(1170) \to \rho\pi$	146 ± 14	142 ± 14
$\pi_2(1670) \to \rho\pi$	80.6 ± 10.8	93.5 ± 13

parameter that captures the strength of flux-tube breaking and, in the wide flux-tube approximation, the function $F(\vec{r},\vec{w}) = 1$ [71]. In the nonrelativistic limit, the Hamiltonian for the decay $P \to D_1 D_2$ reduces to

$$\langle D_1 D_2|\hat{H}|P\rangle = \gamma \int \frac{d^3 r d^3 y}{(2\pi)^{3/2}} e^{i(\vec{p}_1\cdot\vec{r})/2}\Psi_P(\vec{r})\langle\vec{\sigma}\rangle \times (i\vec{\nabla}_1 i\vec{\nabla}_2 + \vec{p}_1)\Psi_1^*\left(\frac{\vec{r}}{2}+\vec{y}\right)\Psi_2^*\left(\frac{\vec{r}}{2}-\vec{y}\right), \tag{B2}$$

where the subscripts P, 1, and 2 represent the parent and the product states respectively, $\langle\vec{\sigma}\rangle$ is the expectation value of the Pauli spin-vector for the $^3P_0$ $\bar{q}q$ pair, and $\vec{p}_1$ is the 3-momentum of the $|D_1\rangle$ state [33]. In the above expression, the wave functions of the states involved are taken as Harmonic oscillator wave functions, which contain the oscillator size parameter β. The two parameters (γ and β) are fitted to the decay widths of the mesons. We have used value $\beta = 0.4$ GeV, as given in Ref. [33]. Since γ is an overall factor multiplying the decay amplitude, the PWAs depend only on the oscillator size parameter. The amplitudes for the decay of the axial-vector and pseudovector mesons to vector and pseudoscalar mesons are given by [33]

$$\mathcal{A}_\ell(1^{++}\to 1^{--}0^{-+}) = \begin{cases} f_S & \ell = 0 \\ -\sqrt{\frac{5}{6}} f_D & \ell = 2 \end{cases} \tag{B3}$$

$$\mathcal{A}_\ell(1^{+-}\to 1^{--}0^{-+}) = \begin{cases} -\frac{1}{\sqrt{2}} f_S & \ell = 0 \\ -\sqrt{\frac{5}{3}} f_D & \ell = 2 \end{cases}, \tag{B4}$$

where

$$f_S = \frac{2^5}{\sqrt{3^5}}\left(1 - \frac{2}{9}\frac{k^2}{\beta^2}\right) \tag{B5}$$

$$f_D = \frac{2^6}{3^4\sqrt{5}}\frac{k^2}{\beta^2}. \tag{B6}$$

For the decays of the pseudotensor mesons, the amplitudes are given by

$$\mathcal{A}_\ell(2^{-+}\to 2^{++}0^{-+}) = \begin{cases} -\frac{2^6}{\sqrt{3^7}}\left(1 - \frac{5}{18}\frac{k^2}{\beta^2} + \frac{1}{135}\frac{k^4}{\beta^4}\right) & \ell = 0 \\ -\sqrt{\frac{2^9 35}{3^{11}}}\frac{k^2}{\beta^2}\left(1 - \frac{4}{105}\frac{k^2}{\beta^2}\right) & \ell = 2 \\ -\sqrt{\frac{2^{13}}{3^{11}7}}\frac{1}{5}\frac{k^4}{\beta^4} & \ell = 4 \end{cases} \tag{B7}$$

$$\mathcal{A}_\ell(2^{-+}\to 1^{--}0^{-+}) = \begin{cases} \frac{1}{2} f_P & \ell = 1 \\ -\sqrt{\frac{7}{5}} f_F & \ell = 3 \end{cases}, \tag{B8}$$

where

$$f_P = \frac{\sqrt{2^{13}}}{3^4}\frac{k}{\beta}\left(1 - \frac{2}{15}\frac{k^2}{\beta^2}\right) \tag{B9}$$

$$f_F = -\frac{2^6}{\sqrt{3^9 35}}\frac{k^3}{\beta^3}. \tag{B10}$$

These amplitudes are related to the decay amplitude through the relation,

$$\mathcal{M} = \frac{\gamma}{\sqrt{\beta}\pi^{1/2}} A_\ell e^{-k^2/16\beta^2}, \tag{B11}$$

where the final exponential factor represents a form factor for the decay process. The ratios of the PWAs obtained using these expressions are listed in Table XIV.

TABLE XIV. Ratios of the PWAs obtained from the $^3P_0$ model compared to the present calculations.

	Present calculation			$^3P_0$ model [33]		
Decay	D/S	G/S	F/P	D/S	G/S	F/P
$a_1(1260) \to \rho\pi$	−0.062			−0.147		
$f_1'(1420) \to K^*K$	−0.0076			−0.026		
$b_1(1235) \to \omega\pi$	0.277			0.284		
$h_1(1170) \to \rho\pi$	0.281			0.207		
$h_1'(1415) \to K^*K$	0.021			0.039		
$\pi_2(1670) \to f_2(1270)\pi$	−0.18	0.0042		0.185	0.0065	
$\pi_2(1670) \to f_2'(1520)\pi$	0.0093	-7.49×10^{-6}		0.00697	2×10^{-5}	
$\eta_2(1645) \to a_2(1320)\pi$	−0.089	0.0011		0.378	0.0026	
$\pi_2(1670) \to \rho\pi$			−0.72			−0.653
$\pi_2(1670) \to K^*K$			−0.447			−0.251
$\eta_2(1645) \to K^*K$			−0.32			−0.193

[1] P. A. Zyla *et al.* (Particle Data Group), Review of particle physics, Prog. Theor. Exp. Phys. **2020**, 083C01 (2020).

[2] G. Amelino-Camelia, F. Archilli, D. Babusci, D. Badoni, G. Bencivenni, J. Bernabeu, R. A. Bertlmann, D. R. Boito, C. Bini, C. Bloise *et al.*, Physics with the KLOE-2 experiment at the upgraded DAϕNE, Eur. Phys. J. C **68**, 619 (2010).

[3] M. Alekseev *et al.* (COMPASS Collaboration), Observation of a $J^{PC} = 1^{-+}$ Exotic Resonance in Diffractive Dissociation of 190 GeV/c π^- into $\pi^-\,\pi^-\,\pi^+$, Phys. Rev. Lett. **104**, 241803 (2010).

[4] M. F. M. Lutz *et al.* (PANDA Collaboration), Physics performance report for PANDA: Strong interaction studies with antiprotons, arXiv:0903.3905.

[5] D. Ryabchikov (VES group and COMPASS Collaboration), Meson spectroscopy at VES and COMPASS, EPJ Web Conf. **212**, 03010 (2019).

[6] R. Aaij *et al.* (LHCb Collaboration), Physics case for an LHCb Upgrade II—Opportunities in flavour physics, and beyond, in the HL-LHC era, arXiv:1808.08865.

[7] H. Al Ghoul *et al.* (GlueX Collaboration), First results from the GlueX experiment, AIP Conf. Proc. **1735**, 020001 (2016).

[8] B. Zihlmann (GlueX Collaboration), GlueX a new facility to search for gluonic degrees of freedom in mesons, AIP Conf. Proc. **1257**, 116 (2010); M. Shepherd, GlueX at Jefferson Lab: A search for exotic states of matter in photon-proton collisions, Proc. Sci. Bormio2014 (**2014**) 004.

[9] G. Mezzadri, Light hadron spectroscopy at BESIII, Proc. Sci. EPS-HEP2015 (**2015**) 423; S. Marcello (BESIII Collaboration), Hadron physics from BESIII, J. Phys. Soc. Jpn. Conf. Proc. **10**, 010009 (2016).

[10] N. Isgur and J. E. Paton, A flux tube model for hadrons in QCD, Phys. Rev. D **31**, 2910 (1985).

[11] S. Godfrey and N. Isgur, Mesons in a relativized quark model with chromodynamics, Phys. Rev. D **32**, 189 (1985).

[12] M. F. M. Lutz, J. S. Lange, M. Pennington, D. Bettoni, N. Brambilla, V. Crede, S. Eidelman, A. Gillitzer, W. Gradl, C. B. Lang *et al.*, Resonances in QCD, Nucl. Phys. **A948**, 93 (2016).

[13] J. R. Pelaez, From controversy to precision on the sigma meson: A review on the status of the non-ordinary $f_0(500)$ resonance, Phys. Rep. **658**, 1 (2016).

[14] E. Klempt and A. Zaitsev, Glueballs, hybrids, multiquarks. Experimental facts versus QCD inspired concepts, Phys. Rep. **454**, 1 (2007).

[15] K. J. Peters, A primer on partial wave analysis, Int. J. Mod. Phys. A **21**, 5618 (2006).

[16] A. Koenigstein, F. Giacosa, and D. H. Rischke, Classical and quantum theory of the massive spin-two field, Ann. Phys. (Amsterdam) **368**, 16 (2016).

[17] F. Divotgey, L. Olbrich, and F. Giacosa, Phenomenology of axial-vector and pseudovector mesons: Decays and mixing in the kaonic sector, Eur. Phys. J. A **49**, 135 (2013).

[18] P. Ko and S. Rudaz, Phenomenology of scalar and vector mesons in the linear sigma model, Phys. Rev. D **50**, 6877 (1994).

[19] G. W. Carter, P. J. Ellis, and S. Rudaz, An effective Lagrangian with broken scale and chiral symmetry: 2. Pion phenomenology, Nucl. Phys. **A603**, 367 (1996).

[20] D. Parganlija, P. Kovacs, G. Wolf, F. Giacosa, and D. H. Rischke, Meson vacuum phenomenology in a three-flavor linear sigma model with (axial-)vector mesons, Phys. Rev. D **87**, 014011 (2013).

[21] A. H. Fariborz, R. Jora, and J. Schechter, Toy model for two chiral nonets, Phys. Rev. D **72**, 034001 (2005).

[22] V. Cirigliano, G. Ecker, H. Neufeld, and A. Pich, Meson resonances, large $N(c)$ and chiral symmetry, J. High Energy Phys. 06 (2003) 012.

[23] A. Pich, Chiral perturbation theory, Rep. Prog. Phys. **58**, 563 (1995).

[24] V. Bernard and U. G. Meissner, Chiral perturbation theory, Annu. Rev. Nucl. Part. Sci. **57**, 33 (2007).

[25] M. R. Schindler, J. Gegelia, and S. Scherer, Electromagnetic form-factors of the nucleon in chiral perturbation theory including vector mesons, Eur. Phys. J. A **26**, 1 (2005).

[26] E. E. Jenkins, A. V. Manohar, and M. B. Wise, Chiral Perturbation Theory for Vector Mesons, Phys. Rev. Lett. **75**, 2272 (1995).

[27] M. Booth, G. Chiladze, and A. F. Falk, Quenched chiral perturbation theory for vector mesons, Phys. Rev. D **55**, 3092 (1997).

[28] C. Terschlüsen and S. Leupold, Renormalization of the low-energy constants of chiral perturbation theory from loops with dynamical vector mesons, Phys. Rev. D **94**, 014021 (2016).

[29] K. S. Jeong, S. H. Lee, and Y. Oh, Analysis of the b_1 meson decay in local tensor bilinear representation, J. High Energy Phys. 08 (2018) 179.

[30] F. Giacosa, A. Koenigstein, and R. D. Pisarski, How the axial anomaly controls flavor mixing among mesons, Phys. Rev. D **97**, 091901 (2018).

[31] G. 't Hooft, How instantons solve the U(1) problem, Phys. Rep. **142**, 357 (1986).

[32] G. A. Christos, Chiral symmetry and the U(1) problem, Phys. Rep. **116**, 251 (1984).

[33] T. Barnes, F. E. Close, P. R. Page, and E. S. Swanson, Higher quarkonia, Phys. Rev. D **55**, 4157 (1997).

[34] A. J. Woss, C. E. Thomas, J. J. Dudek, R. G. Edwards, and D. J. Wilson, b_1 resonance in coupled $\pi\omega$, $\pi\phi$ scattering from lattice QCD, Phys. Rev. D **100**, 054506 (2019).

[35] C. Zemach, Use of angular momentum tensors, Phys. Rev. **140**, B97 (1965).

[36] C. Zemach, Three pion decays of unstable particles, Phys. Rev. **133**, B1201 (1964).

[37] M. Jacob and G. C. Wick, On the general theory of collisions for particles with spin, Ann. Phys. (N.Y.) **7**, 404 (1959).

[38] S. U. Chung, Helicity coupling amplitudes in tensor formalism, Phys. Rev. D **48**, 1225 (1993); **56**, 4419(E) (1997).

[39] S. U. Chung, A general formulation of covariant helicity coupling amplitudes, Phys. Rev. D **57**, 431 (1998).

[40] V. Filippini, A. Fontana, and A. Rotondi, Covariant spin tensors in meson spectroscopy, Phys. Rev. D **51**, 2247 (1995).

[41] J. M. Link *et al.* (FOCUS Collaboration), Study of the $D^0 \to \pi^-\pi^+\pi^-\pi^+$ decay, Phys. Rev. D **75**, 052003 (2007).

[42] S. U. Chung, K. Danyo, R. W. Hackenburg, C. Olchanski, J. S. Suh, H. J. Willutzki, S. P. Denisov, V. Dorofeev, V. V. Lipaev, A. V. Popov *et al.*, Exotic and $q\bar{q}$ resonances in the

$\pi^+\pi^-\pi^-$ system produced in $\pi^- p$ collisions at 18 GeV/c, Phys. Rev. D **65**, 072001 (2002).
[43] K. Ackerstaff *et al.* (OPAL Collaboration), A measurement of the hadronic decay current and the ν_{τ^-} helicity in $\tau^- \to \pi^-\pi^-\pi^+\nu_\tau$, Z. Phys. C **75**, 593 (1997).
[44] H. Albrecht *et al.* (ARGUS Collaboration), Analysis of the decay $\tau^- \to \pi^-\pi^-\pi^+\nu_\tau$ and determination of the $a_1(1260)$ resonance parameters, Z. Phys. C **58**, 61 (1993).
[45] R. Aaij *et al.* (LHCb Collaboration), Observation of $\bar{B}_{(s)} \to J/\psi f_1(1285)$ Decays and Measurement of the $f_1(1285)$ Mixing Angle, Phys. Rev. Lett. **112**, 091802 (2014).
[46] J. J. Dudek, R. G. Edwards, B. Joo, M. J. Peardon, D. G. Richards, and C. E. Thomas, Isoscalar meson spectroscopy from lattice QCD, Phys. Rev. D **83**, 111502 (2011).
[47] Z. Jiang, D. H. Yao, Z. T. Zou, X. Liu, Y. Li, and Z. J. Xiao, "$B^0_{d,s} \to f_1 f_1$ decays with $f_1(1285) - f_1(1420)$ mixing in the perturbative QCD approach, Phys. Rev. D **102**, 116015 (2020).
[48] X. Liu and Z. J. Xiao, Axial-vector $f_1(1285) - f_1(1420)$ mixing and $B_s \to J/\psi(f_1(1285), f_1(1420))$ decays, Phys. Rev. D **89**, 097503 (2014).
[49] S. Stone and L. Zhang, Use of $B \to J/\psi f_0$ Decays to Discern the $q\bar{q}$ or Tetraquark Nature of Scalar Mesons, Phys. Rev. Lett. **111**, 062001 (2013).
[50] M. Ablikim *et al.* (BESIII Collaboration), Observation of $h_1(1380)$ in the $J/\psi \to \eta' K\bar{K}\pi$ decay, Phys. Rev. D **98**, 072005 (2018).
[51] H. Y. Cheng, Revisiting axial-vector meson mixing, Phys. Lett. B **707**, 116 (2012).
[52] A. V. Anisovich, C. J. Batty, D. V. Bugg, V. A. Nikonov, and A. V. Sarantsev, A fresh look at $\eta_2(1645)$, $\eta_2(1870)$, $\eta_2(2030)$ and $f_2(1910)$ in $\bar{p}p- > \eta 3\pi^0$, Eur. Phys. J. C **71**, 1511 (2011).
[53] A. Koenigstein and F. Giacosa, Phenomenology of pseudotensor mesons and the pseudotensor glueball, Eur. Phys. J. A **52**, 356 (2016).
[54] D. Barberis *et al.* (WA102 Collaboration), A Study of the $\eta\pi^+\pi^-$ channel produced in central pp interactions at 450 GeV/c, Phys. Lett. B **471**, 435 (2000).
[55] D. Barberis *et al.* (WA102 Collaboration), A study of the $KK\pi$ channel produced centrally in pp interactions at 450 GeV/c, Phys. Lett. B **413**, 225 (1997).
[56] D. M. Li and E. Wang, Canonical interpretation of the $\eta_2(1870)$, Eur. Phys. J. C **63**, 297 (2009).
[57] P. R. Page, E. S. Swanson, and A. P. Szczepaniak, Hybrid meson decay phenomenology, Phys. Rev. D **59**, 034016 (1999).
[58] B. Povh and J. Hufner, Systematics of strong interaction radii for hadrons, Phys. Lett. B **245**, 653 (1990).
[59] M. F. M. Lutz and W. Weise, Sizes of hadrons, Nucl. Phys. **A518**, 156 (1990).
[60] C. Amsler and F. E. Close, Is $f_0(1500)$ a scalar glueball?, Phys. Rev. D **53**, 295 (1996).
[61] V. C. Shastry and K. B. Vijaya Kumar, Effects of finite size of constituent quarks on nucleon–nucleon interaction, J. Phys. G **46**, 065101 (2019).
[62] J. Vijande, P. Gonzalez, H. Garcilazo, and A. Valcarce, Screened potential and the baryon spectrum, Phys. Rev. D **69**, 074019 (2004).
[63] T. Wolkanowski, M. Sołtysiak, and F. Giacosa, $K_0^*(800)$ as a companion pole of $K_0^*(1430)$, Nucl. Phys. **B909**, 418 (2016).
[64] C. A. Baker, C. J. Batty, K. Braune, D. V. Bugg, N. Djaoshvili, W. Dünnweber, M. A. Faessler, F. Meyer-Wildhagen, L. Montanet, I. Uman *et al.*, Confirmation of $a_0(1450)$ and $\pi_1(1600)$ in $\bar{p}p \to \omega\pi^+\pi^-\pi^0$ at rest, Phys. Lett. B **563**, 140 (2003).
[65] A. Tayduganov, E. Kou, and A. Le Yaouanc, The strong decays of K_1 resonances, Phys. Rev. D **85**, 074011 (2012).
[66] S. Jafarzade, A. Koenigstein, and F. Giacosa, Phenomenology of $J^{PC} = 3^{--}$ tensor mesons, Phys. Rev. D **103**, 096027 (2021).
[67] T. Wang, Z. H. Wang, Y. Jiang, L. Jiang, and G. L. Wang, Strong decays of $D_3^*(2760)$, $D_{s3}^*(2860)$, B_3^*, and B_{s3}^*, Eur. Phys. J. C **77**, 38 (2017).
[68] C. T. Johnson and J. J. Dudek (Hadron Spectrum Collaboration), Excited J^{--} meson resonances at the SU(3) flavor point from lattice QCD, Phys. Rev. D **103**, 074502 (2021).
[69] F. Giacosa, A. Okopińska, and V. Shastry, A simple alternative to the relativistic Breit–Wigner distribution, Eur. Phys. J. A **57**, 336 (2021).
[70] R. Kokoski and N. Isgur, Meson decays by flux tube breaking, Phys. Rev. D **35**, 907 (1987).
[71] P. Geiger and E. S. Swanson, Distinguishing among strong decay models, Phys. Rev. D **50**, 6855 (1994).